International Journal of Modern Physics B Vol. 2, No. 6 (1988) 1331–1379

HIGH T_c STUDIES IN SVERDLOVSK*

B.N. GOSHCHITSKII,† V. L. KOZHEVNIKOV‡ and M. V. SADOVSKII*
†*Institute for Metal Physics,*‡ *Institute for Chemistry,** Institute for Electrophysics,
USSR Academy of Sciences, Ural Branch, *Sverdlovsk, USSR*

Received 19 March 1988

This review reports the main experimental results on superconducting lattice and electron properties of high-temperature superconductors of the type $La_{2-x}Sr_xCuO_4$ and $YBa_2Cu_3O_7$ obtained at three institutes of the Ural Branch of the USSR Academy of Sciences in Sverdlovsk. Special attention is paid to investigations of structural phase transitions, heat capacity, optic and magnetic properties, NMR relaxation and the role of radiation disordering under the influence of fast neutron irradiation. In conclusion, a brief review of possible theories to explain high-temperature superconductivity in metal oxides is given.

Introduction

The publication of pioneer papers by Bednorz and Müller[1] and Chu *et al.*[2] stimulated extended studies on synthesis and physical properties of new high-temperature superconductors at three institutes of the Ural Branch of the USSR Academy of Sciences in Sverdlovsk. In February 1987 we synthesized single phase samples of $La_{2-x}Sr_xCuO_{4-y}$ with maximum $T_c \simeq 36.5$ K. At the end of March the samples of 1-2-3 based on yttrium were obtained, with $T_c \simeq 93$ K. At the same time we started investigating temperature dependences of electron and lattice parameters such as electrical resistance, thermoelectric power, Hall effect, magnetization and magnetic susceptibility, heat capacity, velocity and absorption of longitudinal ultrasound, high-frequency behavior etc. The following methods were used to investigate lattice and electron structures and the phonon spectrum of superconducting ceramics:

— elastic and inelastic thermal neutron scattering,
— NMR, EPR,
— Mössbauer spectroscopy,
— optical reflectance and Raman scattering,
— X-ray emission spectroscopy,
— X-ray diffraction,
— electron microscopy.

The effect of disordering on critical parameters of superconducting ceramics

*The present review is based on the report of one of the authors (M. V. Sadovskii) made during the *Adriatico Research Conference on High Temperature Superconductors, 5–8 July, 1987 Trieste, Italy, enriched by some new data.*

was investigated by different methods on the samples irradiated by fast neutrons ($E \geq 1$ meV) in a wide range of fluences both in the normal and superconducting states. The present review reports the most important data, from our viewpoint, obtained by different groups of the Ural scientists.

1. The $La_{2-x}Sr_xCuO_{4-y}$ System

The compounds investigated within the concentration range (x=0.02 + 0.4) were synthesized[3] from Cu oxides and La with doping by Sr-carbonate according to the following reaction

$$\left(1 - \frac{x}{2}\right) La_2O_3 + x\,SrCO_3 + CuO = La_{2-x}Sr_xCuO_{4-y} + x\,CO_2$$

using the standard ceramic technology. The X-ray-phase analysis was used to control whether the reaction was complete or not. The interaction between the components was studied with thermo-analyzer in air, heating rate being 10 grad/min.

Besides, the compounds of the composition $x = 0.17$ doped by different elements (La was substituted by Ce, Cu by Co, O by F)[4] were also synthesized.

1.1. Superconducting properties

Figure 1 shows the dependence of T_c on Sr concentration[3] determined by a four-contact resistivity method. The maximum T_c value determined by the midpoint of the transition was 36.5 K for $x = 0.17$. For x less or greater than this value T_c decreases, while full transition width increases. For $x \leq 0.06$ and $x = 0.4$ there was no superconductivity above 1.7 K.

Electrical resistance of the samples changed from units to tens of mΩ/cm at $T > T_c$. In the samples with Sr concentration $x = 0.02 + 0.08$ within the temperature range $T \lesssim 100$ K negative temperature coefficient of resistivity (TCR) was observed. For $x = 0.1 + 0.3$ TCR is positive. In the system of solid solutions under study, superconductivity persisted up to 38 K (Fig. 1). The temperature derivative of the upper critical field determined by the midpoint of the transition was ~ 2 T/K. On the average T_c determined by inductive measurements was 5 K lower than by resistive ones while the transitions were broader. In the best samples the concentration of the superconducting phase accounted for 70–90%, $T_c = 37$ K, full width of the resistive transition $\Delta T_c \simeq 4$ K. The strongest degradation of superconductivity takes place on substitution of the Cu atoms (e.g. after 5% replacement by Zn atoms we did not observe superconductivity up to 1.7K), F doping decreases T_c less markedly (from 37 to 22 K on 8% substitution of the O atoms). Substitution of La by Ce also results in T_c decreasing and transition broadening.

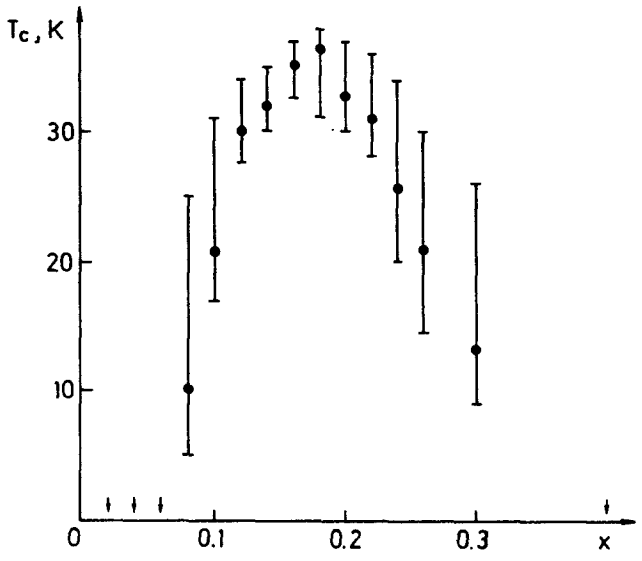

Fig. 1. Dependences of T_c and ΔT_c upon Sr concentration. The straws show full width of superconducting transition. Vertical arrows show that superconducting transition was not observed with decreasing temperature to 1.7 K[3].

1.2. Heat capacity and the phonon spectrum

Heat capacity of the samples with $x = 0.17$ was investigated. It was measured by the adiabatic method within the temperature range 3–300 K with an error not more than 0.5% and within the interval 3–50 K in magnetic fields from 0.4 to 8 T, the random error being 0.4% (non-excluded systematic error does not exceed 1%)[4,5]. The measurements in magnetic fields were carried out at Kurchatov Institute for Atomic Energy (Moscow).

Figure 2 shows the temperature dependence of heat capacity C_p. Within the range $T \simeq 37$ K the jump was observed correspondent to superconducting transition, the value of which being $\Delta C_p / T_c \simeq 1$ mJ/g.atom K^2. This accounts for ~ 1.5% of the total heat capacity of the sample. Within the whole temperature range above T_c heat capacity monotonically depends on temperature. For comparison we measured heat capacity of the $La_{1.9}Sr_{0.1}CuO_{4-y}$ sample ($T_c \simeq 29$ K). The results are shown by dotted lines in Fig. 2. It is seen that the jump is less marked here (the superconducting transition is more smeared), while the phonon heat capacities are practically the same for both samples indicating the identity of the phonon spectra of the compounds with different T_c (37 and 29 K).

Figure 3 depicts heat capacity data measured in different magnetic fields. At any value of the field the jump shifts towards the lower temperatures with increasing field. The critical temperature of the superconducting transition

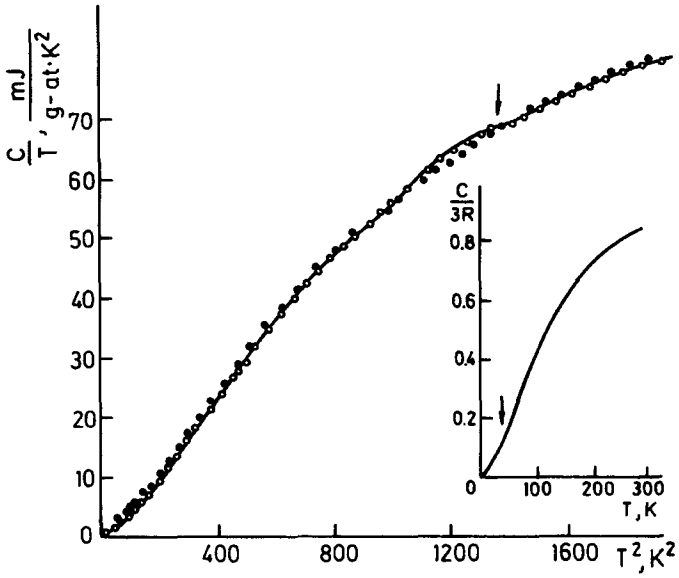

Fig. 2. Heat capacity C_p/T vs. T^2 : o for $La_{1.83}Sr_{0.17}CuO_{4-y}$, • for $La_{1.9}Sr_{0.1}CuO_{4-y}$ ($T_c = 29$ K). The arrows show the distribution of jumps in heat capacity.[5]

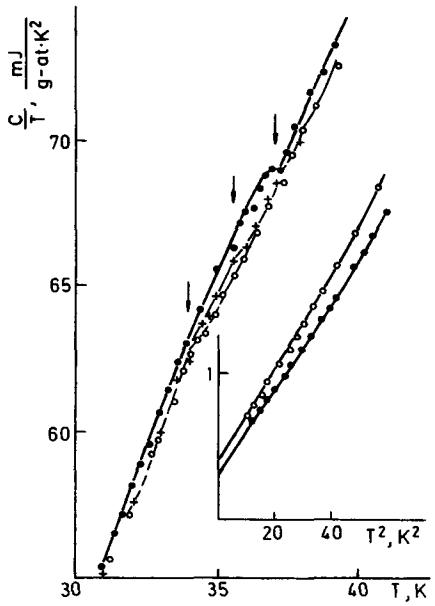

Fig. 3. Heat capacity of $La_{1.83}Sr_{0.17}CuO_{4-y}$ in different magnetic fields: o means $H=0$, + – 4 T, • – 8 T. The arrows show jumps in heat capacity.[5]

determined by the middle of heat capacity jump was 37 K, 35.5 K and 33.9 K in zero field, 4 T and 8 T, respectively. This allows us to estimate the value of dH_{c2}/dT in the vicinity of T_c: $dH_{c2}/dT = 2.6\ T/\text{K}$.

In the low-temperature range $T < 7$ K the heat capacity behaves like $C_p = \beta T^3 + \gamma T\beta$ corresponds to Debye temperature $\theta_D = 370 + 20$ K, while the linear term is small (γ does not exceed 0.2 mJ/ g.atom K^2, being within experimental error). Hence, at low temperatures heat capacity is determined by phonons. This is in agreement with the data on superconducting transition measured by an inductive method showing the 100% content of the superconducting phase. The insertion in Fig. 3 depicts heat capacity in the low-temperature range in magnetic field. At $T < 7$ K heat capacity is well described by the law $C_p = \beta T^3 + \gamma_H T$, the value of β does not practically depend upon the value of the magnetic field and corresponds to Debye temperature 390 K. The coefficient γ_H depends strongly upon magnetic field increasing from 0.3 in zero field to 0.43 mJ/g.atom K^2 in the field of 8 T. The fact that zero field γH is not equal to zero indicates that the sample contains some amount of the normal (non-superconducting) phase.

Using the data obtained we estimated the order of magnitude for electron heat capacity coefficient γ for the sample of $La_{1.83}Sr_{0.17}CuO_{4-y}$ in normal state. The relation $\gamma = \dfrac{\partial \gamma_H}{\partial H} H_{c2}(0)$, where $\dfrac{\partial \gamma H}{\partial H} = 0.016$ mJ/g.atom K^{2}T and $H_{c2}(0) \simeq 66$ T gives $\gamma \simeq 1$ mJ/g.atom K^2. Evaluation of γ according to the values of residual electric resistance $\rho_o \simeq 1$ mΩ cm and $H'_{c2} \simeq 2$T/K provides $\gamma \simeq 0.2$–0.5 mJ/g.atom K^2. These estimates coinciding in order of magnitude with the observed jump and its transformation in magnetic field indicate the bulk superconductivity in the sample.

To clarify lattice dynamics we investigated the phonon spectrum using inelastic neutron scattering and Raman scattering.[4,5] Inelastic neutron scattering was measured with time-of-flight spectrometer with a cryogenic source of cold neutrons at the IR-8 reactor of the Institute for Atomic Energy (Moscow). The mean energy of the incident neutrons was $E = 4.4$ meV.

Double differential neutron scattering cross-section was measured at room temperature. After introducing ordinary corrections experimental data were treated in noncoherent approximation. Then the spectra measured at different angles of neutron scattering were summarized. Figure 4 thus shows the obtained total function of energy distribution of lattice vibrations, $G(E)$.[5] The $G(E)$ function has the limiting energy of 88 meV. The high-energy "tail" above this limit, seen in the figure, is likely to be due to the processes of multiphonon neutron scattering and anharmonic lattice vibrations. The low-energy part of the spectrum (up to ~ 10 meV) is described by quadratic dependence $G(E) \sim E^2$. The Debye temperature determined from this part of spectral distribution turned out to be ~ 380 K. The shape of the phonon spectrum is in qualitative agreement with the temperature dependence of heat capacity shown in Fig. 2.

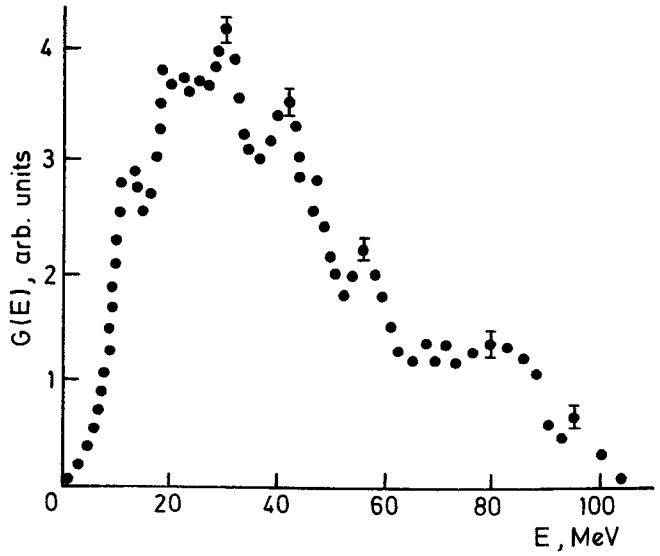

Fig. 4. $G(E)$ for the samples of $La_{1.83}Sr_{0.17}CuO_{4-y}$.[5]

Spectral distribution shows a number of peaks at the energies of 12, 20, 30, 40, 56 and 80 meV. The analogous structure of the phonon spectrum was observed in Ref. 6. The peak at 12 meV is likely to be connected with transverse acoustic phonons. It may account for the departure of temperature dependence of heat capacity from the law $C(T) \sim T^3$ for $T \simeq 10$ K. This peculiarity as well as the behavior of heat capacity described above is supported by the data of Ref. 7. The two high-energy maxima at 56 and 80 meV correspond, probably, to vibrations of the oxygen atoms having different coordination with respect to atoms of Cu.

Raman scattering provides qualitatively the same picture for the energy distribution of lattice vibration (Fig. 5).[5] Due to argon laser heating ($\lambda = 5145$ Å, 200 MW) the local temperature of the sample was 100–150 K higher than the temperature of the holder and was estimated from the relation between the Stokes and anti-Stokes components. The resolution was ~0.5 meV. The scattered light was not analyzed. The peaks observed in the spectrum correspond to the energies of 19, 27, 5 and 52 meV and are likely to result from three (of four possible Raman-active modes) optic vibrations of the La and O atoms distributed out of the planes containing the chains of Cu-O-Cu. This is supported by some decrease in line widths and their high-frequency shift with decreasing temperature. The peculiarities observed in Raman spectra agree with the data of inelastic neutron scattering and microcontact spectroscopy.[8]

In Ref. 9 heat capacity and phonon spectrum of the compounds $La_{2-x}Sr_xCuO_{4-y}$ with different x concentration ($x = 0$, 0.06 and 0.17) were investigated. It was found that y increases with increasing x. Qualitatively the form of the $G(E)$ function changes negligibly for different concentrations: the distribution of low-

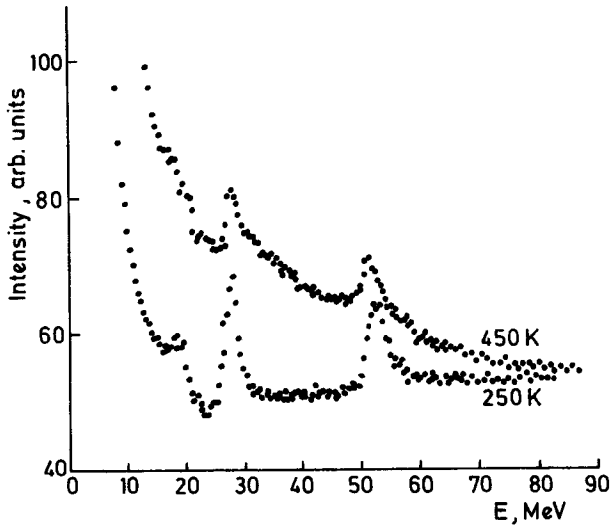

Fig. 5. Raman spectrum of $La_{1.83}Sr_{0.17}CuO_{4-y}$ for two temperatures. Apparatus solution is 0.5 meV.[5]

energy ($E < 50$ meV) spectrum peculiarities practically does not change, while the peculiarities within the range of $E > 50$ meV shift towards the lower energies.

1.3. Lattice transformations

At room temperature solid solutions of the system $La_{2-x}Sr_xCuO_{4-y}$ with $x \geqslant 0.1$ have the K_2NiF_4 structure (Fig. 6). For $x \leqslant 0.1$ the orthorhombic distortion of this structure for the stoichiometric La_2CuO_4 ($T_m < 533$ K) was observed.[10–12] The problem of the structural transition and its connection with high-temperature superconductivity was already discussed.[13]

The detailed measurements of the temperature dependences of the crystal lattice parameters of this system for $0 \leqslant x \leqslant 0.4$ were made in Refs. 14, 15. For convenience the authors described the orthorhombic lattice using pseudomonoclinic cell with the following parameters:

$$a = \frac{1}{2}\sqrt{a_o^2 + a_o^2}\,,\ c = c_o\,,\ \gamma = \operatorname{arctg}\frac{b_o}{a_o}\,.$$

In this case, in tetragonal phases $\gamma = 90°$, while the shift of γ from 90° is the measure of orthorhombic distortions.

Figures 7 and 8 show the temperature dependences of the lattice parameters and the volume of pseudomonoclinic cell $V = a^2c \sin\gamma$ for the samples with different compositions. It is found that neither distribution of the diffraction maxima nor the ratios intensities change while going through T_c. As a result there

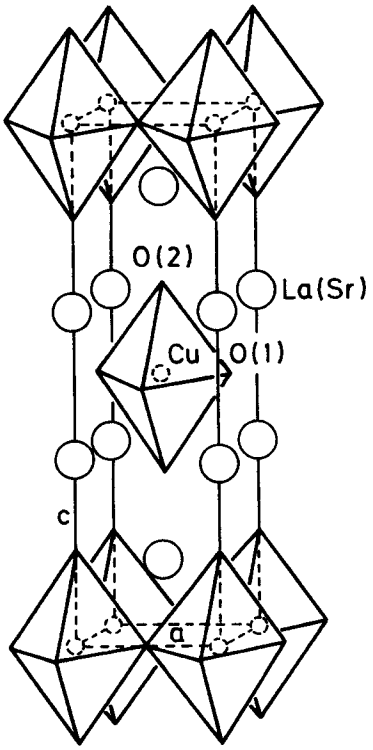

Fig. 6. The crystal structure of $La_{2-x}Sr_xCuO_{4-y}$.

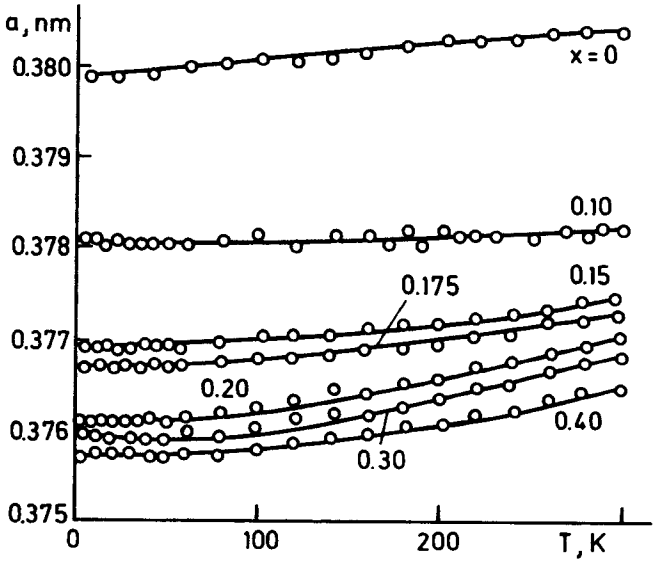

Fig. 7. Temperature dependences of the lattice parameter a[14].

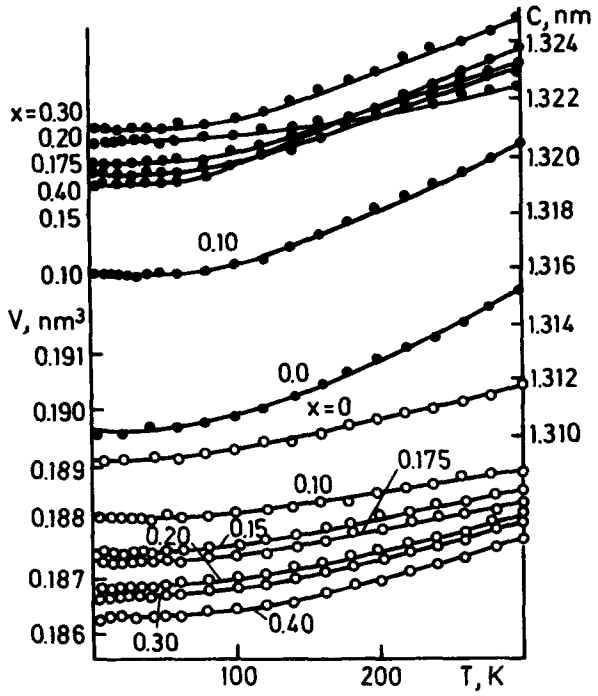

Fig. 8. Temperature dependences of the lattice parameter C and the volume of the pseudomonoclinic cell for the samples of different compositions.[14]

are no anomalies on the curves $a(T)$, $c(T)$ and $V(T)$ with an accuracy up to linear deformations of the order of 10^{-4}.

Figure 9 shows the temperature dependences of the orthorhombic distortions, i.e. the values of γ-90° for the compositions with $0 \leqslant x \leqslant 0.175$. It is seen that in La_2CuO_4, T_m for the structural transition from orthorhombic to tetragonal phase is 590 K. The character of phase transition was studied for the composition $La_{1.9}Sr_{0.1}CuO_{4-y}$. The profile of the line (310) was measured on an individual single-crystal particle obtained while grinding the sintered and recrystallized ceramics. In spite of the essential improvement of accuracy in determining distortions there was no jump in parameter γ-90° during the transition, i.e. the structural transition is apparently of the second order.

Figure 10 depicts the concentration dependences of pseudomonoclinic cell parameters a and c, its volume V and γ-90° distortion. Extrapolation of γ-90° vs. x to zero allows the finding of the critical value x_{cr} at which the temperature of the structural transition T_m tends to zero.

The temperature and concentration dependences of structural characteristics obtained together with the measured T_c allows reliable enough picture of the (T, x)-phase diagram for solid solutions of $La_{2-x}Sr_xCuO_{4-y}$ (see Fig. 11) to be

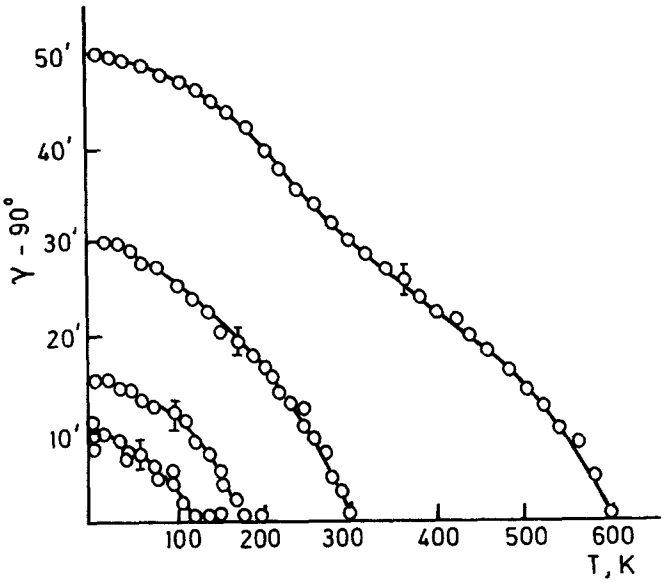

Fig. 9. Temperature dependences of the orthorhombic distortions γ-90° for compounds with different compositions.[14]

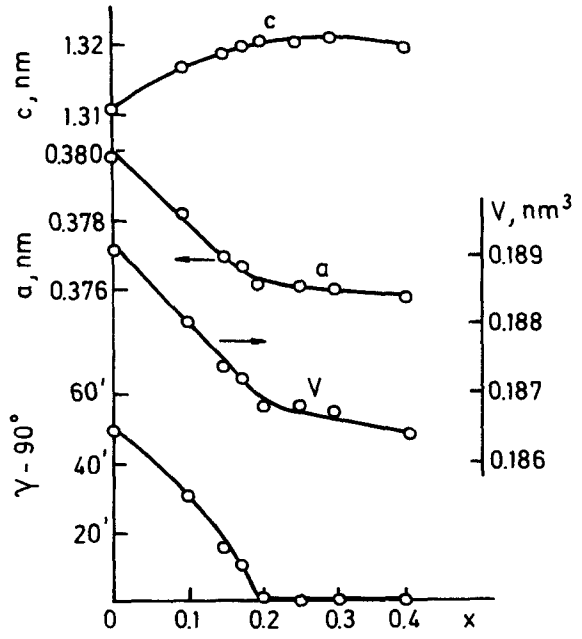

Fig. 10. Concentration dependences of the parameters of the pseudomonoclinic unit and its volume at T=5 K.[14]

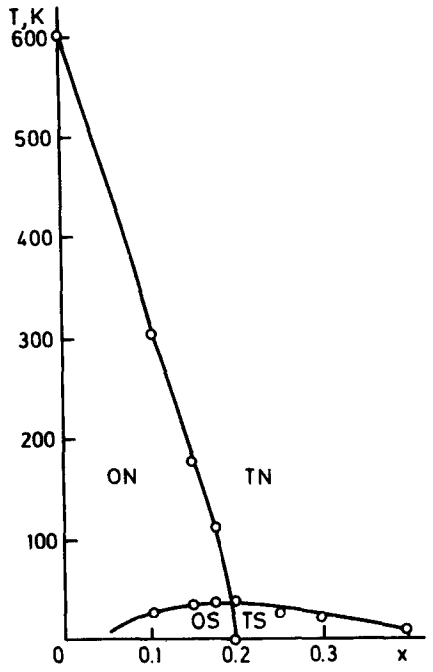

Fig. 11. The phase diagram for solid solutions of $La_{2-x}Sr_xCuO_{4-y}$. The signs T and O show the tetragonal and orthorhombic phases, and S and N show the superconducting and normal ones.[14]

obtained. The fact of approximate coincidence of T_c and T_m in the concentration range with maximum T_c is of interest. The same phase diagram was obtained in Ref. 16.

The superconducting state is found both in orthorhombic and tetragonal phases. The authors of Refs. 14, 15 believe the orthorhombic distortions unlikely to be connected with high-T_c behavior.

In Ref. 17 the temperature dependences of velocity and longitudinal supersound absorption and thermal linear expansion coefficient of $La_{1.88}Sr_{0.17}CuO_{4-y}$ were measured in the range 4.2–300 K. The data obtained support the picture of the tetragonal-orthorhombic structural transition in the La-Sr ceramics. All of the measured parameters show some peculiarities near T_c and well-marked anomalies at 136 K indicating the occurrence of the structural transition for this compound. The results are given in Figs. 12, 13, 14.

The conclusions made in Refs. 14, 15, 17 concerning the occurrence of this structural transition are also confirmed by the results of direct electron-microscope and electron-diffraction measurements.[18]

1.4. Electron band structure

Information concerning the electron structure of $La_{1.83}Sr_{0.17}CuO_{4-y}$ was obtained from X-ray emission spectra investigations and self-consistent band-structure calculations.[19] X-ray emission spectra of CuL_α, OK_α and $CuK_{\beta 5}$, $LaL_{\beta 5}$

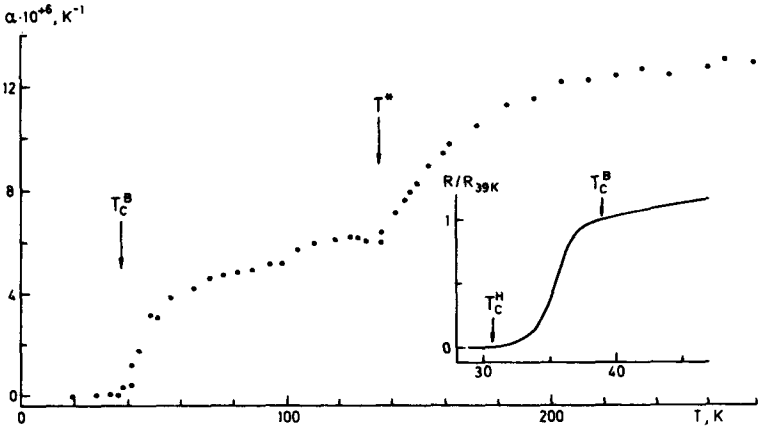

Fig. 12. Temperature dependence of the linear thermal expansion coefficient. The insert shows the variation of relative electrical resistance $R/R_{39\,K}$ within the range of superconducting transition.[17]

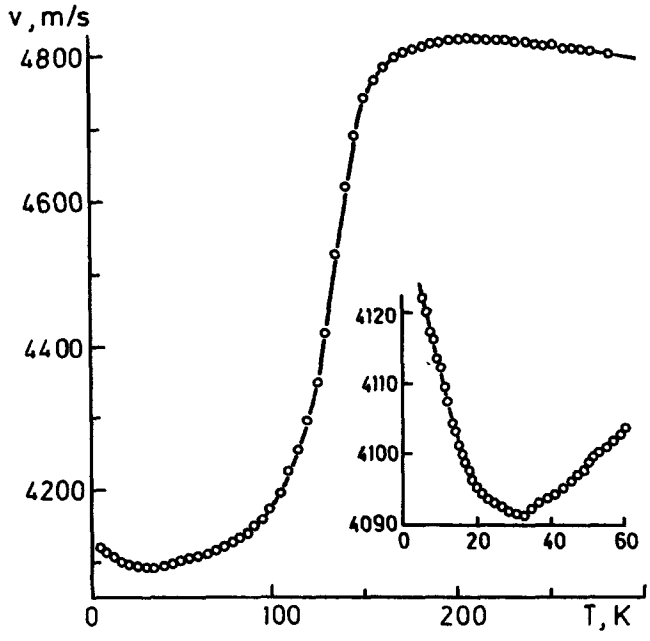

Fig. 13. Temperature dependence of the longitudinal ultra-sound velocity.[17]

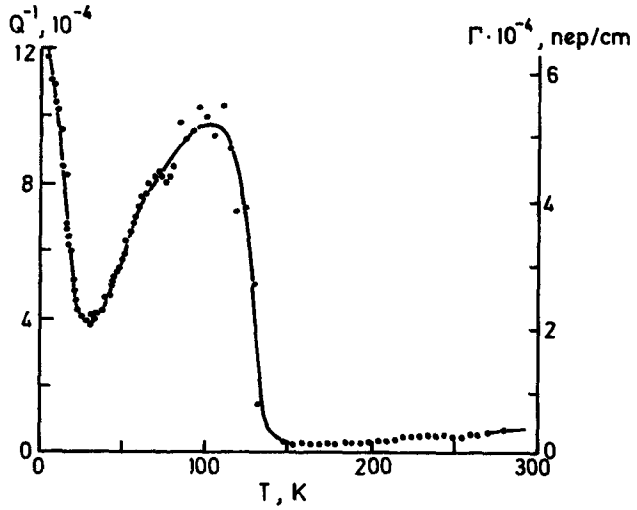

Fig. 14. Temperature dependences of the sample quality and longitudinal ultra-sound absorption.[17]

were studied. The spectra were compared in one and the same energy scale taking into account the difference between the energies of Cu2*p* and O1*s* core levels measured with photoelectron spectroscopy. Figure 15 depicts measurement results and band-structure calculations.

The electron structure was calculated by a self-consistent LMTO-method. The calculations were made for La_2CuO_4 with a tetragonal crystal structure and lattice parameters of $La_{1.83}Sr_{0.17}CuO_4$. The valence of copper in these compounds is mainly two, while the atomic states Cu3*d* and O2*p* are close in energy and cause rather strong hybridization. As a result the valent band is strictly divided into bonding and anti-bonding sub-bands. La_2CuO_4 has a layered structure where Cu-O octahedrons are connected through oxygen atoms O_{xy} each of which, in its turn, is connected with two atoms of Cu. The O_z-type oxygen atoms are connected with only one atom of Cu, the bond being perpendicular to the plane of the layer. Atoms of La fill the space between the layers. The results of the calculation show that the La5*d* band is above the Fermi level and the Cu3*d* and O2*p* states play the main role in forming the valence band. In this case the O_{xy}-type atoms due to strong hybridization with Cu3*d* split into two subbands. The 2*p* states of the O_z-type atoms are split to become much weaker, their maximum falls into the gap of the O_{xy}-type band. As a result the total density of states O2*p* does not show marked splitting into two subbands and this is reflected in OKα spectrum for $La_{1.83}Sr_{0.17}CuO_4$. In general the calculation results are in good agreement with the band structure described in Refs. 20, 21.

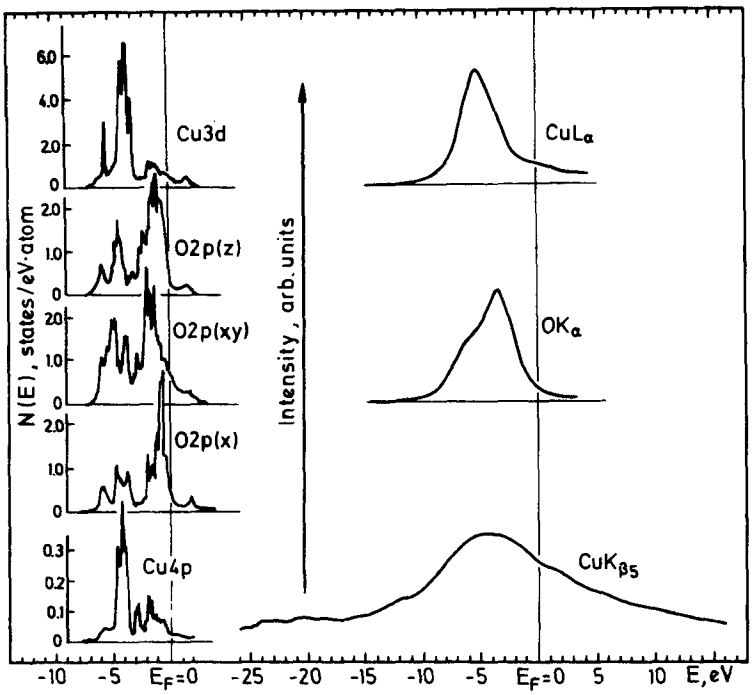

Fig. 15. X-ray emission spectra for $La_{1.83}Sr_{0.17}CuO_{4-y}$ and the calculation results of the electron structure of La_2CuO_4.[19] On the left partial density of states are shown, on the right their correspondent spectra. $CuK_{\beta 5}$, $LaL_{\beta 5}$, OK_α, CuL_α correspond to transitions ($1s$–$4p$), ($2p3/2$–$5d$), ($1s$–$2p$) and ($2p$–d), respectively. O_{2px} is the partial density of the $2p$ oxygen atoms located in the layer of Co-O octahedrons. O_z corresponds to the oxygen atoms located over the layer.

1.5. Kinetic properties

According to Hall effect measurements on the samples with $x = 0.04$, 0.10 and 0.17[4,22] within the range 4.2–77 K hole conductivity predominates in the normal phase. Concentrations p and hole-mobilities R_6 calculated from Hall coefficient and conductivity are as follows:

$$p = 6.10^{17}\,\mathrm{cm}^{-13}\,,\ R_6 \simeq 1\,\mathrm{cm}^2/\mathrm{V.s.}\ \text{for}\ x = 0.04\,;$$

$$p \simeq 10^{21}\text{–}10^{27}\,\mathrm{cm}^{-3}\,,\ R_6 = 1\text{–}6\mathrm{cm}^2/\mathrm{V.s.}\ \text{for}\ x = 0.10\ \text{and}\ 0.17\,.$$

The hole type of conductivity is supported also by thermoelectric power measurements made on the sample with $x = 0.17$.[23] For $T > T_c$ thermoelectric power is positive corresponding to the sign of Hall effect. This implies that holes are predominant charge carriers. Figure 16 shows temperature dependences of

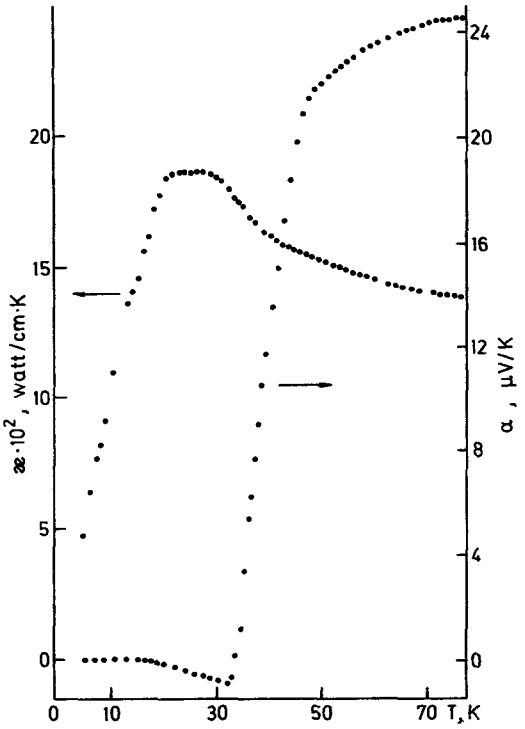

Fig. 16. Temperature dependence of thermoelectric power α and heat conductivity æ for $La_{2-x}Sr_xCuO_4$, $x=0.17$.[23]

thermoelectric power and heat conductivity. They are typical of superconductors near T_c.

Knowing hole concentration from Hall effect p = (5–10). 10^{21} cm^{-3} one may estimate the effective mass of the hole m using the general formula for the case of degenerate gas of carriers:

$$\alpha = \frac{2\pi^{2/3}}{3^{5/3}} \frac{k_\beta^2 T}{l^2 h^2} \frac{(r+1)}{p^{2/3}} m .$$

The value of r which describes energy dependence of hole relaxation time is within the limits from 0 to 2 for different scattering mechanisms. The estimates show that at $T > T_c$ m/m_0 changes from $\simeq 1$ to $\simeq 7$ in the interval 34–45 K for r = 1 and $p=5.10^{21}$ cm^{-3} while for $p=1.10^{22}$cm^{-3} it changes from $\simeq 2$ to $\simeq 11$. The data obtained in Refs. 22, 23 are in good agreement with the results of other authors.[24–26]

Besides, interesting hysteresis and time phenomena occurring in unusual resistive state of the La-Sr ceramics at weak magnetic fields were investigated in Ref. 22. The authors believe these phenomena to be associated with the transition to superconducting glass state (see also Ref. 27).

Rapid Commun.
in High T_c

2. The $RBa_2Cu_3O_{7-y}$ System

The most convenient way to synthesize $RBa_2Cu_3O_{7-y}$ type copper oxides is to obtain them from R_2O_3, CuO oxides and $BaCO_3$ carbonate. The correspondent mixtures of needed stoichiometry were ground under ethanol to obtain homogeneous mass, dried and pressed in pellets then quenched at 900–930° for 6–10 hours (the first stage). At high-temperature contact of reactionary mixtures with Pt, strong enough reduction was observed. Hence, we used the pellets of synthesized material as a protection substrate and synthesized the remaining part of the mixture. Then the pellets were crashed, ground, again pressed and annealed at 900–930° for 6–10 hours (the second stage). The second stage was repeated to obtain single-phase product. X-ray phase analysis was used to control phase composition. Before the final sintering the samples were ground, screened through a screen with a hole diameter of $\sim 50\ \mu$m, pressed under the pressure of $\sim$ 10 kbar in pellets of 2–3 mm in thickness and 8–12 mm in diameter and annealed at 930–950° for 6–10 hours. Then they were cooled down to room temperature with the velocity of 60–100 grad/min (the third stage).

To oxidize the samples they were sealed in a heated quartz crucible filled with oxygen under the pressure of 1–2 atm. and exposed to additional thermal treatment at 930–950°C for 6–10 hrs. Then the crucible was cooled to 650–700°C at a rate of 60–100 grad/min and kept at this temperature for 6–10 hrs. After this procedure the samples were cooled to 450–500°C hardened for 6–10 hrs and then cooled to room temperature (the fourth stage).

The necessity to restrict the temperature on the first stage is caused by the formation of non-equilibrium eutectics melting at $T \geqslant 930$°C, containing the initial nonreacted reagents and intermediate synthesis products. Decreasing temperature during synthesis results in a great amount of the phases $BaCuO_2$ and $RBACuO_5$ in the correspondent stoichiometric relations and sharp slowing down of the rate of formation of the phase $RBa_2Cu_3O_{7-y}$. Annealing at maximum premelting temperatures, the samples with 90–95% of theoretical density consisting of well-formed microcrystals $\sim 50\ \mu$m in size were obtained.

2.1. *Superconducting properties*

Single phase compounds $RBa_2Cu_3O_{7-y}$ (R = Y, Nd, Sm, Eu, Gd, Er, Tm, Ho, Yb, Lu, Dy) isostructural with $YBa_2Cu_3O_{7-y}$ and crystallizing in orthorhombic crystal system[28,29] are obtained with the above method. $PrBa_2Cu_3O_{7-y}$ crystallizing in tetragonal system is an exception. The samples synthesized under the same conditions were used to measure the superconducting transition temperature T_c by inductive and resistive methods. Using inductive measurements we determine bulk concentrations of superconducting C_s and normal C_n phases estimating them from the inductance of the coil calibrated against the standard Pb and Nb

samples, the accuracy of concentration measurements was ~ 5%. Bulk concentration of superconducting phase determined by inductive method is the upper limit for real fraction of superconducting phase (due to possible screening effects). All of the samples obtained under given conditions had concentration of the superconducting phase more than 95% with an exception of $NdBa_2Cu_3O_{7-y}$ where $C_s \simeq 30\%$. The curves for superconducting transition obtained by inductive method (Figs. 17 and 18) show the features typical of all the compounds $RBa_2Cu_3O_{7-y}$. Firstly, the onset of superconductivity is at ~ 94 K; secondly, the transitions are extended to low-temperature range. In the samples with Er, Sm, Ho, Gd, and Y a complete transition occurs above 60 K. The resistive transition curves are narrower for all of the samples. For example, in compounds with Y, Er, Ho, Sm full transition occurs at $T > 90$ K. At $\simeq 90$ K normal phase concentrations in these compounds account for ~80%. This is in agreement with percolation models with non-correlated distribution of normal and superconducting phases over the sample volume.

Resistive measurements show that in magnetic fields above $0.6T$ the end of the superconducting transition shifts towards the lower temperature range in correlation with full transition width determined by an inductive method (Figs. 17 and 18).

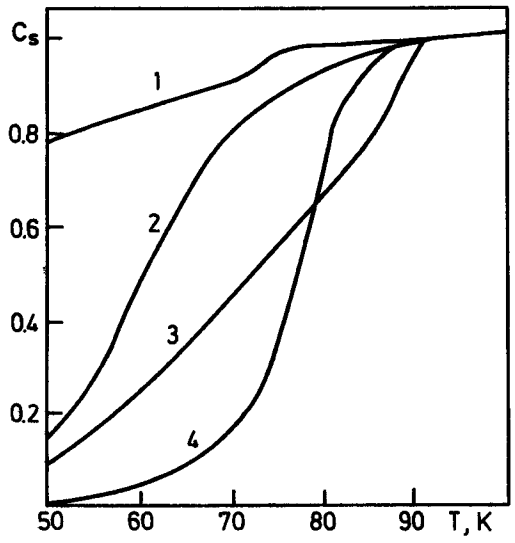

Fig. 17. Normal phase concentrations C_n for $RBa_2Cu_3O_{7-y}$ determined by variation of coil inductance depending on temperature T[28] : curve 1 – R=Nd, curve 2 – R=Tm, curve 3 – R=Yb, curve 4 – R=Lu.

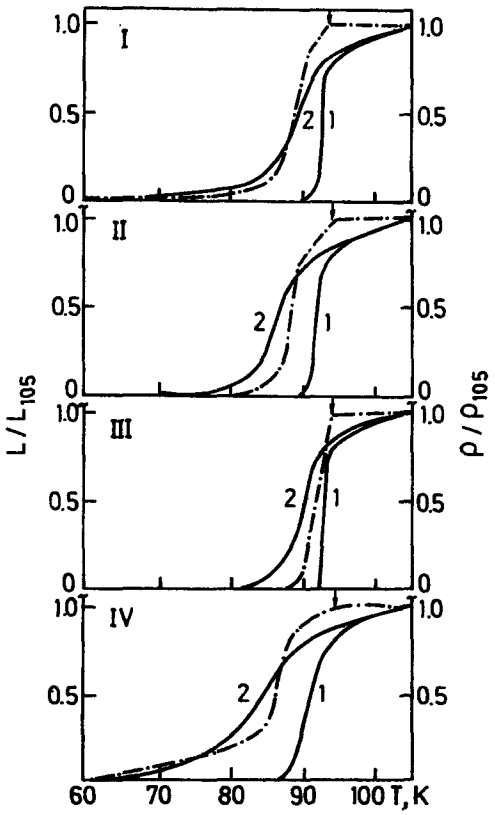

Fig. 18. Dependence of reduced electrical resistance ρ/ρ (105 K) without magnetic field (curve 1), in magnetic field of 5.1 T(curve 2) and the reduced values of coil inductance L/L (105 K) shown by dash-dot line for $RBa_2Cu_3O_{7-y}$[28]: R is Er, Sm, Ho, Gd for diagrams I, II, III and IV, respectively.

The temperature derivative of the upper critical field $\left.\frac{dH_{c2}}{dT}\right|_{T=T_c} \equiv H'_{c2}$ depends both upon the transition width without magnetic field and the choice of the ρ value, at which it is determined. For example, in compounds with Er, H'_{c2} equals 3 T/K, 1.4 T/K and 0.6 T/K for $\rho = 0.8\,\rho$ (105 K), $\rho = 0.5\,\rho$ (105 K) and $\rho = 0.2\,\rho$ (105 K), respectively. From Table 1, it follows that the larger the transition width the less the value of H'_{c2}: decrease in the transition width from 20 to 3.5 K obtained on changing the thermodynamic conditions during the synthesis of $HoBa_2Cu_3O_{7-y}$ is accompanied by an increase in H'_{c2} from 1.0 to 1.7 T/K. Electrical resistance for compounds with Y, Gd, Sm, Ho, Lu, Tm, Er, Dy depends on temperature in the following way: with cooling from room temperature to some T_m (shown by an arrow in Fig. 18) decreases linearly. Below T_m the curve ρ

(T) shifts down from linear dependence going smoothly to superconducting transition. The T_m value varies from ~ 180 K to ~ 125 K for compounds with Lu and Y, respectively. Application of a magnetic field does not affect the behavior of $\rho(T)$ at $T \geqslant 105$ K (Fig. 19). An essential spread of ρ (100 K) values (from 0.4 to 2–3 mΩ cm) at close values of the ratio ρ(300 K)/ρ(110 K) is likely to be connected with different porosity of the samples. Hence, one should treat electron heat capacity factor γ estimated from the data on H'_{c2} and ρ with caution.

In general superconducting properties of the samples under study are in good agreement with the results obtained by other authors (see for example, Refs. 30–32).

2.2. *Heat capacity and phonon spectrum*

Temperature dependences of heat capacity $Cp(T)$ for $RBa_2Cu_3O_{7-y}$ (R = Y, Er, Ho) compounds were investigated within the temperature range 3–300 K.[29,33] At low temperatures in compounds with R = Er, Ho some peculiarities in heat capacity were observed. Most likely they are connected with splitting of $4f$ levels of the rare-earth ions by a crystal field of ligands (Fig. 20). In $YBa_2Cu_3O_{7-y}$ as well as in $La_{1.03}Sr_{0.17}CuO_{4-y}$ temperature dependences at $T < 10$ K are described by relation $Cp = \gamma T + \beta T^3$ (Debye temperature $\theta_D = 375 + 10$ K, $\gamma \leq$ 0.2mJ/g.at.K^2). At $T > 200$ K heat capacities for Y(Er, Ho)$Ba_2Cu_3O_{7-y}$ and $La_{1.83}Sr_{0.17}O_{4-y}$ coincide with an accuracy of ~ 1% indicating that at high enough

Table 1. Parameters of $RBa_2Cu_3O_{7-y}$.

Parameter	Y	Nd	Sm	Eu	Gd	Ho	Er	Tm	Yb	Lu	Dy
T_c^L, K	91.8	60	88.2	78	86.0	92.0	89.0	86.0	73.0	76.5	90.5
T_c^R, K	92.7	81.6	92.2	82.3	90.4	93.3	92.6	92.3	90.9	89.0	93.2
H'_{c2}, T/K	1.6	0.6	1.2		0.9	1.7	1.4				
ρ(300)/ρ(100)	2.3	1.2	2.3	1.5	2.2	2.5	1.8	2.2	1.9	2.4	1.7
ρ100K,mOhm cm	0.4	1.0	0.7	1.7	0.64	0.7	2.0	1.2	1.4	0.9	0.8
ΔT_c^L, K	5.7	44.5	5.0	18	23.5	3.5	6.0	15.5	37	17.5	7.5
ΔT_c^R, K	0.6	15.3	2.2	2.5	5.0	0.6	1.7	1.0	12.2	9.0	1.0

T_c^L and T_c^R are midpoint temperatures of superconducting transition determined by inductive and resistive methods respectively. H'_{c2} is the derivative of the upper critical field, determined at the midpoint of the resistive transition.

ΔT_c^L and ΔT_c^R are the transition widths (10–90%) obtained by inductive and resistive methods respectively.

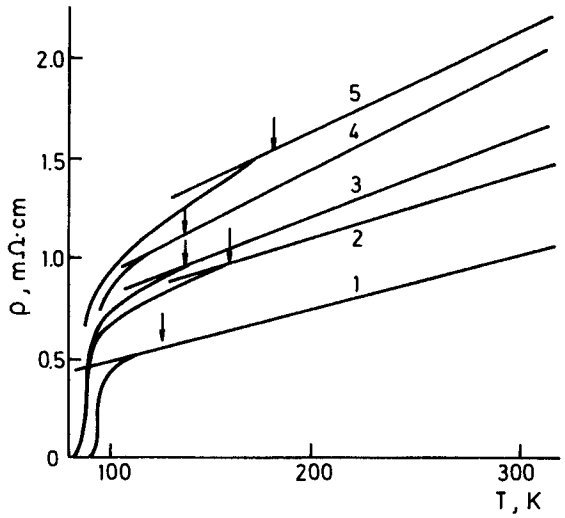

Fig. 19. Temperature dependence of electrical resistance ρ for $RBa_2Cu_3O_{7-y}$[28]: R=Y (curve 1), R=Gd (curve 2), R=Sm (curve 3), R=Ho (curve 4), R=Lu (curve 5).

frequencies their phonon spectra are close. Figure 21 shows the jumps of heat capacity at the superconducting transition: $\frac{\Delta C}{T_c} = 3 \pm 0.3$ mJ/g.at.K^2 in $RBa_2Cu_3O_{7-y}$ (in $La_{1.83}Sr_{0.17}CuO_{4-y} \simeq 1.7 \pm 0.3$mJ/g.at.K^2). Analogous jumps of heat capacity were observed in Ref. 34.

Recent experiments on inelastic thermal neutron scattering support the above interpretation of low-temperature anomalies of heat capacity.

Phonon spectrum of $YBa_2Cu_3O_{7-y}$ was investigated at room temperature on a time-of-flight spectrometer at Kurchatov Institute for Atomic Energy (Moscow).[35] Figure 22 shows the depedence of the total frequency distribution of oscillating states $G(E)$ for $YBa_2Cu_3O_{7-y}$. Here for comparison $G(E)$ for $La_{1.83}Sr_{0.17}CuO_{4-y}$ is given.[5] From a comparison of the spectra it is seen that the limiting energies coincide. The most important discrepancies appear at $E >$ 40 meV pointing to total hardening of the spectrum in $YBa_2Cu_3O_{7-y}$ in comparison with La ceramics. The peak observed in $YBa_2Cu_3O_{7-y}$ at 12 meV is essentially supressed. The authors believe it to be connected with low density of states for oxygen oscillations within this energy range.

Raman scattering in $RBa_2Cu_3O_{7-y}$ (R = Y, Sm, Ho) was investigated in Ref. 36. The results are shown in Fig. 23. Seven lines were observed in the spectra of the single phase samples at frequencies 152, 206, 270, 332, 440, 505 and 586 cm^{-1}. Group-theory analysis made for the space group P_{mmm} taking into account small

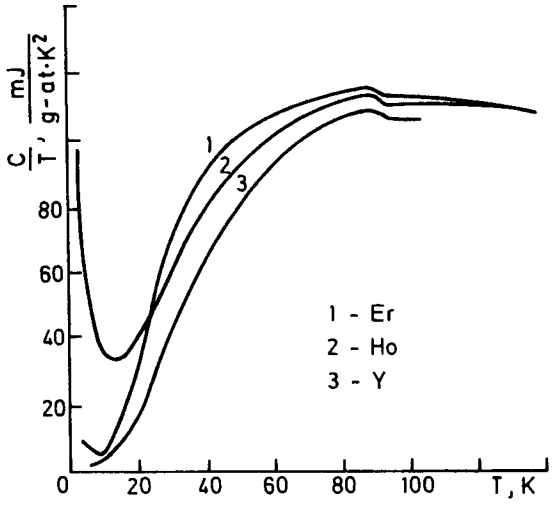

Fig. 20. Temperature dependence of C/T for $RBa_2Cu_3O_{7-y}$ (R=Y, Er, Ho).[33]

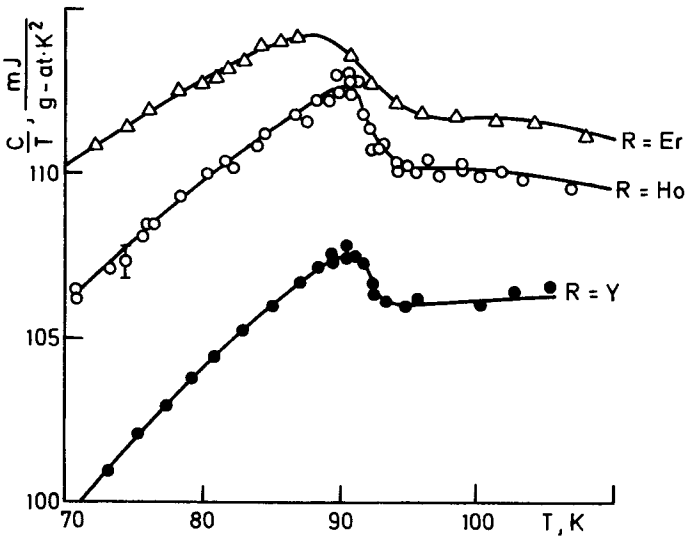

Fig. 21. Heat capacity jumps during the superconducting transition for $RBa_2Cu_3O_{7-y}$ (R=Y, Er, Ho).[33]

orthorhombic lattice distortions gives qualitatively the same spectrum of Raman active vibrations. Cooling the sample to 75 K does not result in essential changes of frequencies and line widths.

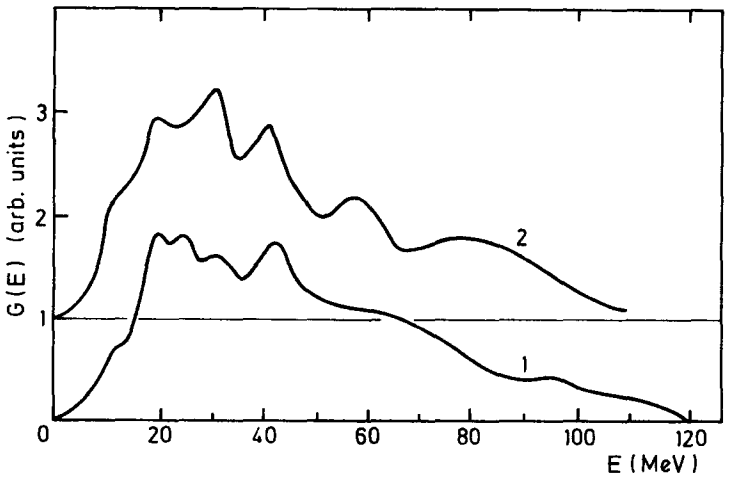

Fig. 22. The $G(E)$ function[35]: $YBa_2Cu_3O_{7-y}$ (curve 1), $La_{1.83}Sr_{0.17}CuO_{4-y}$ (curve 2)

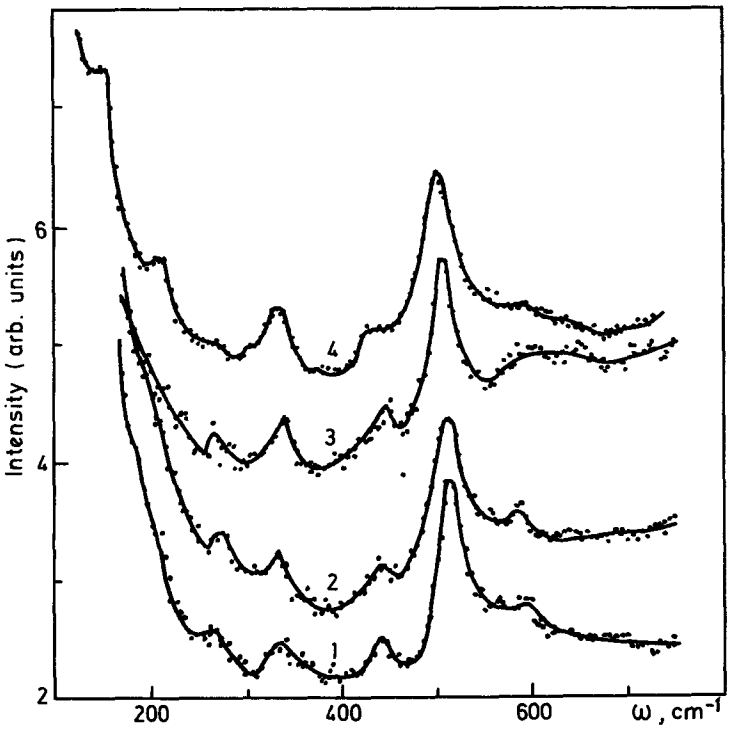

Fig. 23. Raman spectra for $RBa_2Cu_3O_{7-y}$ (R = Y, Sm, Ho).[36]

High intensity of the line at 505 cm^{-1} suggests that this mode or group of ıodes is connected with rather strong deformation potential (strong electron-honon interaction).

.3. *Crystal and electron structure*

Crystal structure of the $RBa_2Cu_3O_{7-y}$ compounds was investigated with X-ray ıd neutron diffraction methods. Figure 24 shows its orthorhombic unit ;ll.[37,38,39,40] As an example Fig. 25 shows the neutron diffraction pattern for $rBa_2Cu_3O_{7-y}$ at room temperature ($\lambda = 1.515$Å, $\Delta d/d \simeq 0.5\%$).[38]

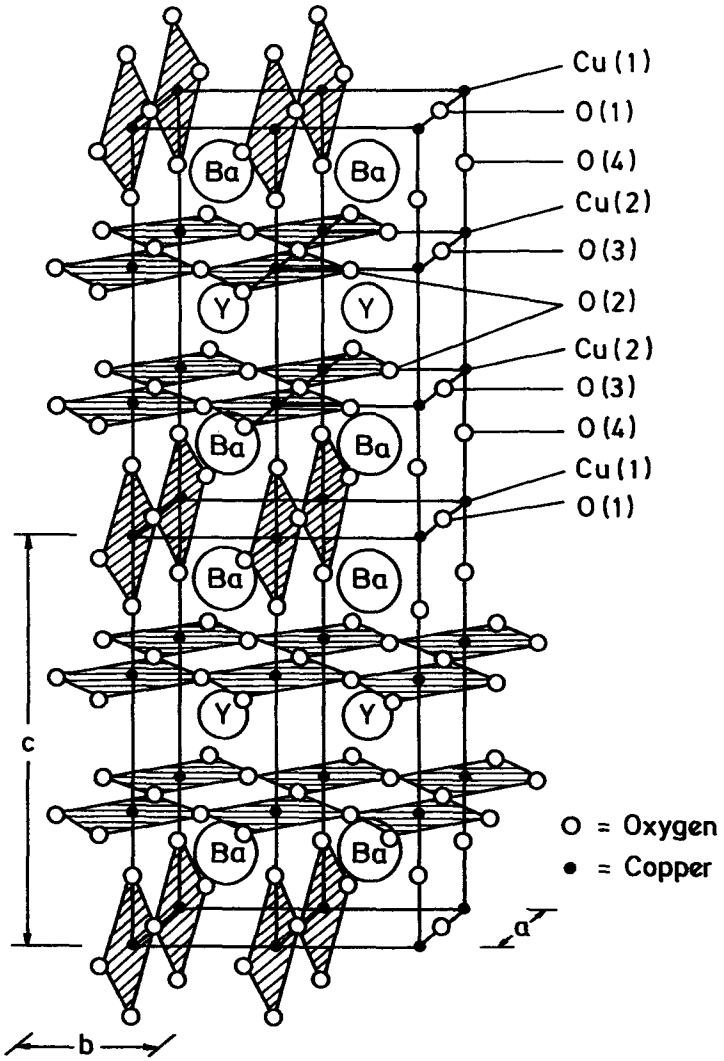

Fig. 24. Orthorhombic unit cell for $YBa_2Cu_3O_{7-y}$ (a,b,c).

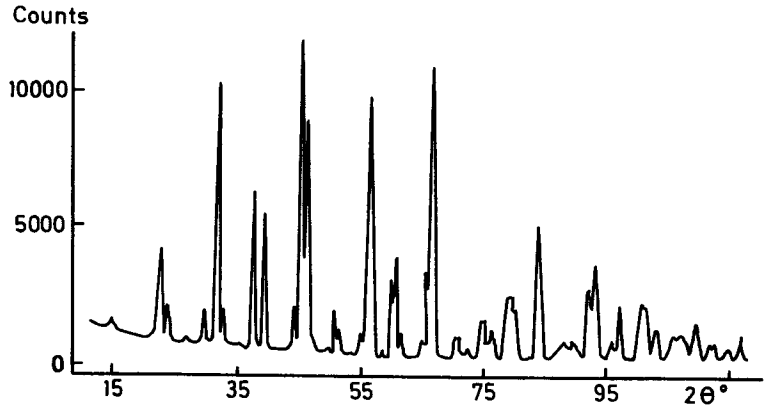

Fig. 25. Neutron diffraction pattern at room temperature for $ErBa_2Cu_3O_{7-y}$.[38]

All the lines are indexed in rhombic unit cell (the space group $P_{mmm} - D^1_{2h}$). The atoms are in the following positions: Ba in $2f$(1/2 1/2 ± z), Er in $1h$ (1/2 1/2 1/2), Cu1 in $1a$ (0 0 0), Cu2 in $2Q$ (0 0± z), O1 in $2Q$ (0 0 ± z), O2 in $2s$ (1/2 O ± z), O3 in $2r$ (0 1/2 ± z), O4 in $1e$ (0 1/2 0) and O5 in $1b$ (1/2 0 0).

Table 2. Coordinates (Z) of atoms and thermal factors (B) for elements at different lattice sites for $ErBa_2Cu_3O_{7-y}$

	Ba	Er	CuI	Cu2	01	02	03	04
Z	0.1822(14)			0.3578(9)	0.158(1)	0.381(1)	0.376(2)	
B	0.78(4)	0.51(6)	0.90(10)	0.51(6)	1.1(1)	0.51(6)	0.94(5)	1.75(6)

This structure agrees with the data of other authors (see, for example, Refs. 41, 42). In Ref. 37 the change of the lattice parameters a,b,c for three compounds $RBa_2Cu_3O_{7-y}$ (R = Y, Er, Ho) was investigated in the temperature interval 5–650 K. Figure 26 shows the temperature dependences of parameters a,b,c and degrees of tetragonality (b/a-1) for these compounds. Absolute errors of measurements are as follows: $\Delta a = \Delta b = 0.003$ Å, $\Delta c = 0.01$ Å, Δ (b/a-1) = 0.0015. As seen from the figure unlike $La_{2-x}Sr_xCuO_{4-y}$ the orthorhombic structure is retained through the whole temperature interval under study, (b/a-1) increases with increasing T. At room temperature structural transition was observed with decreasing oxygen concentration: for $7-y < 6.3$ the samples $YBa_2Cu_3O_{7-y}$ have tetragonal structures.[43]

Electron structures of $YBa_2Cu_3CuO_{7-y}$ was investigated in Ref. 19. $YBa_2Cu_3O_{7-y}$ is characterized by a two-band structure of OK_α spectrum (Fig. 27), while in $La_{1.83}Sr_{0.17}CuO_{4-y}$ the band has no well-marked structure (Fig. 15). For $YBa_2Cu_30_{7-y}$ the intensity maximum of the CuL_α band coincides with the low-

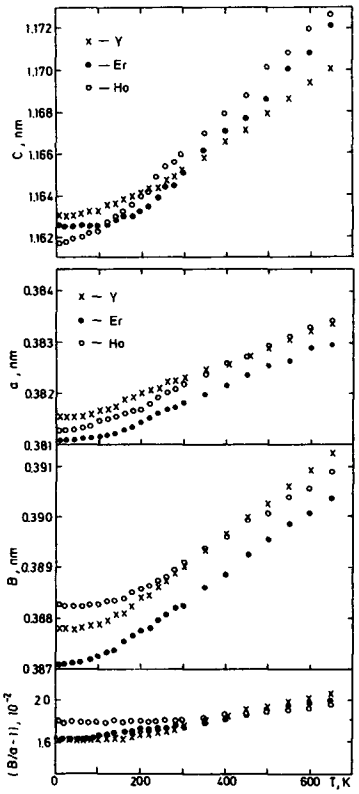

Fig. 26. Temperature dependences of lattice parameters and degrees of tetragonality for $RBa_2Cu_3O_{7-y}$ (R = Y, Er, Ho).[37]

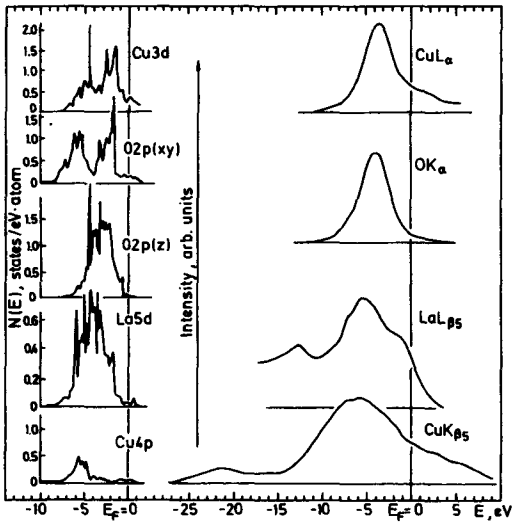

Fig. 27. The X-ray emission spectra for $RBa_2Cu_3O_7$ and the calculation results of the $YBa_2Cu_3O_{7-y}$ electron structure.[19] On the left partial densities of atomic states are shown, on the right their correspondent spectra. CuL_α $CuK_{\beta5}$ and OK_α correspond to transitions ($2p$–$3d$), ($1s$–$4p$) and ($1s$–$2p$), respectively, The O_x type atoms are located along the chains of Cu-O squares. The O_{xy} atoms are located on the base of the pyramid of five oxygen atoms surrounding an atom of Cu. The O_z type atom is located at the summit of the pyramid.

energy subband of the OK_α spectrum. For $La_{1.83}Sr_{0.17}CuO_{4-y}$ intensity maxima of the CuK_α and OK_α bands practically coincide. Thus, for both compounds Cu3*d* and O2*p* states are greatly hybridized to form the band with complex distribution of density of states. From a comparison of Figs. 15 and 26 it is seen that in $La_{1.83}Sr_{0.17}CuO_{4-y}$ the contribution of the *d*-states prevails in the high-energy part of the band including Fermi level. In contrast in $YBa_2Cu_3CuO_{7-y}$ the *d*-states are mainly concentrated in a low-energy part, while near the Fermi level the O2*p* states predominate.

Electron structure of $YBa_2Cu_3O_{7-y}$ was calculated with self-consistent LMTO method. The crystal structure of this compound is rather complex. It has two unequivalent Cu sites and four types of oxygen atoms. The calculation results show that the main difference from La_2CuO_4 consists in strong hybridization of 3*d* states and splitting of partial density of O2*p* states into two subbands for all of the four types of oxygen atoms. This is accounted for by the fact that in this structure each of the oxygen atoms is coupled with two atoms of Cu. Hence, OK_α spectra of $YBa_2Cu_3O_{7-y}$ distinctly show the two band structures. According to the analysis of the density of states for different types of the oxygen atoms the O_x type atoms are characterized by relatively low broadening of antibonding subband. This broadening results from the oxygen-oxygen interaction which is the weakest for the O_x type atoms. Therefore, Cu-O-Cu interactions are the strongest for O_x atoms providing the possibility for one-dimensional electron subsystems are large oscillation amplitudes for oxygen atoms along the directions perpendicular to these chains. Qualitatively the same picture of partial densities of states follows from the calculations by Mattheis and Hamman.[44]

2.4. *Kinetic properties*

Hall effect ($T=160$ K) and thermoelectric power ($4.2 \leq T \leq 185$ K) were measured on the sample of $YBa_2Cu_3O_{7-y}$.[45,46] As in the case of $La_{1.83}Sr_{0.17}Cu_3O_{7-y}$ the signs of Hall effect and thermoelectric power indicate the hole conductivity. The analogous result was obtained in Ref. 30. The hole concentration estimated by Hall effect was $p = 2.5 \times 10^{22}\,\mathrm{cm}^{-3}$. Figure 28 shows temperature dependence of thermoelectric power. On going to a normal state thermoelectric power increases sharply from zero to + (10–15) μV/grad and continues to grow up to $T=110$ K above which it falls. Non-monotonic change especially the decrease of $\alpha(T)$ was observed under the conditions of strong electron scattering $h_h \geqslant \epsilon_F$ (τ is the relaxation time, ϵ_F is Fermi energy) which is obvious from the experimental value of Hall mobility $R_6 \simeq 0.5\mathrm{cm}^2/\mathrm{sec}$. Using these data and simple theoretical scheme with narrow peak in the density of states near ϵ_F[46] one may roughly evaluate the effective hole mass: for $T=100$ K, $-m \lesssim 10\ m_0$ (where m_0 is the free electron mass).

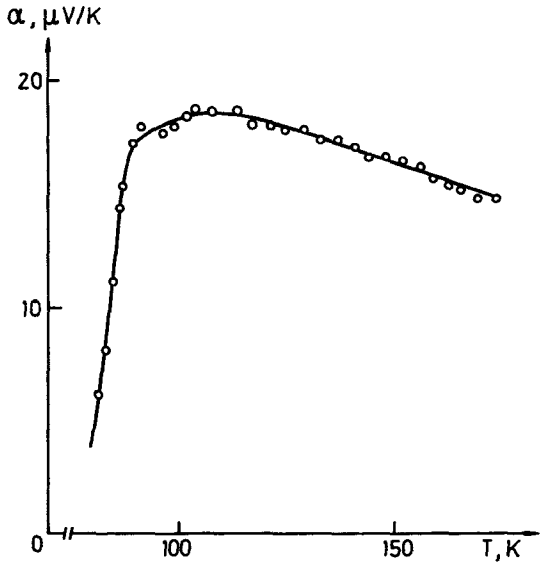

Fig. 28. Temperature dependence of thermoelectric power.[46]

2.5. *Magnetic properties*

Magnetic properties of $RBa_2Cu_3O_{7-y}$ were measured[38,39] with vibrational magnetometer in the range 4.5–300 K in magnetic fields of 25–2000 kA/m that is much less than $H_{c2}(0)$. Magnetic susceptibility χ measured on $RBa_2Cu_3O_{7-y}$ (R = Er, Ho) shows that above 100 K temperature dependence of χ is well-described by Curie-Weiss law with paramagnetic Curie temperature $\theta = +(8\pm2)$K for both compositions (Fig. 29). Below T_c χ depends upon the value of an applied magnetic field. In low fields in the vicinity of T_c there is a sharp maximum of a reverse susceptibility (the insert in Fig. 29 shows the temperature dependence of $1/|\chi|$ for $ErBa_2Cu_3O_{7-y}$ in a field of 40 kA/m). Analogous behavior was observed for $HoBa_2Cu_3O_{7-y}$. With the increase of the applied magnetic field a maximum of an inverse susceptibility deforms and shifts towards the lower temperatures. For $T < T_c$ magnetization curve depends strongly upon magnetic pre-history of the sample (cooling in zero or non-zero magnetic field). In particular, as it follows from Fig. 29, there is no maximum susceptibility in a magnetic field of 800 kA/m within the whole temperature interval and the sample is in a paramagnetic state. The values of magnetic moments of Er and Ho ions calculated from Curie constants are 8.5 μ_B and 9.7 μ_B, respectively, that is little bit lower than the theoretical values μ_{eff} for the free ions (9.58 μ_B and 10.61 μ_B). At room temperature magnetization curves have no hysteresis and depend linearly upon magnetization of the field.

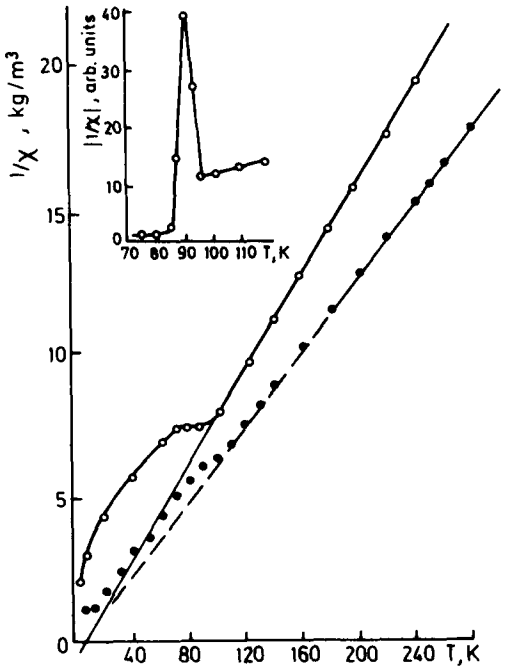

Fig. 29. Temperature dependence of a reverse susceptibility. The measurement field is 800 kA/m[38]: ○ for $ErBa_2Cu_3O_{7-y}$, • for $HoBa_2Cu_3O_{7-y}$. The insert depicts the absolute value of a reverse susceptibility for $ErBa_2Cu_3O_{7-y}$ in the field of 40 kA/m near T_c.

From Fig. 30 it is seen that at 4.5 K in small field (less than 430 kA/m for Er and 260 kA/m for Ho systems) magnetization curves are typical of superconductors. The increase in an applied magnetic field up to 120 kA/m (approximately H_{c1}) leads to magnetization increase in diamagnetic region. Within the interval of magnetic fields of 430–1280 kA/m and 260–1280 kA/m for the samples with Er and Ho, respectively, magnetization curves have the dependence characteristic of paramagnets. The analogous results were obtained by a number of other authors.[47–49] For $T = 4.5$ K (see Fig. 30) there are no signs of magnetic ordering. It was found[50–52] that the temperatures of magnetic (antiferromagnetic) ordering are essentially lower in these systems.

Figure 31a shows magnetization curves for the superconductor $ErBa_2Cu_3O_{7-y}$ at 77 K. The sample was cooled down to the temperatures of measurement without an external magnetic field. It is seen that the magnetization curve has a hysteresis behavior. In this case a pronounced diamagnetic effect is seen in small fields. At $H > 120$ kA/m a positive constituent is seen, magnetization dependence upon the field is linear up to 1600 kA/m. On the decrease of a field at first stage a

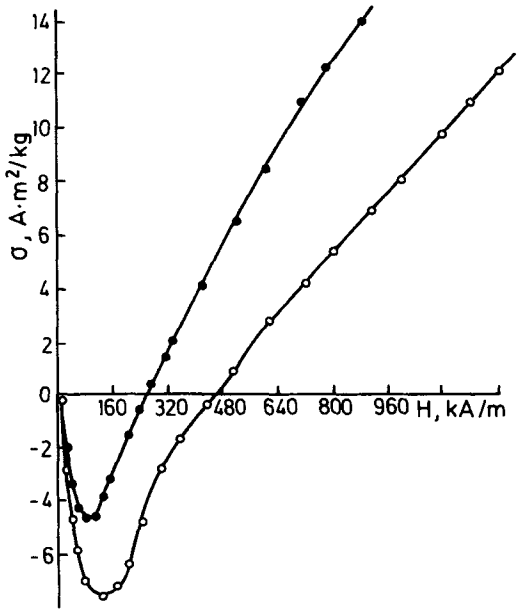

Fig. 30. The dependence of specific magnetization upon the value of an applied magnetic field at 4.5 K[38]: ○ denotes $ErBa_2Cu_3O_{7-y}$, • denotes $HoBa_2Cu_3O_{7-y}$.

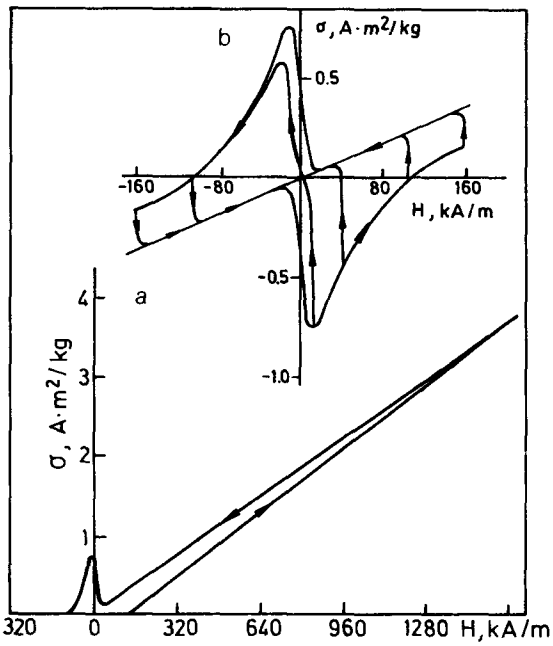

Fig. 31. Magnetization curve for $ErBa_2Cu_3O_{7-y}$ at 77 K (a), individual hysteresis loops for $ErBa_2Cu_3O_{7-y}$ at 77 K (b).[38]

reverse character of remagnetization is observed and then beginning from $H >$ 1360 kA/m hysteresis appears. Diamagnetic contribution begins to predominate only in the field of $\lesssim$ 10 kA/m. To analyse magnetization curves in some details we investigated partial hysteresis loops (Fig. 31b). For $H <$ 100 kA/m, on changing the sign of the field magnetization falls on a limiting cycle corresponding to diamagnetic behavior. For H > 100 kA/m the transition to a limiting cycle is observed with a slight field decrease. The hysteresis picture observed at 77 K may be explained as direct superposition of strong paramagnetism due to the rare-earth ions and a typical diamagnetic hysteresis loop of type II superconductors. The hysteresis disappears on heating the sample to $T > T_c$, maximum (minimum) in small fields corresponds to H_{c1}, in high fields the hysteresis disappears at $H \simeq H_{c2}$. The striking feature of the system under study is that superconducting state persists in the magnetized sample (an applied field $H >$ 100 kA/m).

2.6. Optical properties

In Refs. 45, 53 reflection spectra of the samples of $YBa_2Cu_3O_{7-y}$ were investigated at 4.2 and 300 K in a far IR region from 100 to 300 cm^{-1} with a Fourier spectrometer. The technique allowed to measure the spectral dependence of a reflectivity with an accuracy of the order of 1%. These spectra are shown in Fig. 32. (T_c = 93 K). It is seen that both spectra have five peaks at 200, 230, 280, 310 and 570 cm^{-1}. At 4.2 K the spectrum shows an extra feature for 460 cm^{-1}.

Location of the peaks at 200, 230, 280, 310 and 570 cm^{-1} is correlated with the values of the phonon frequencies in Raman spectra, and is presumably connected

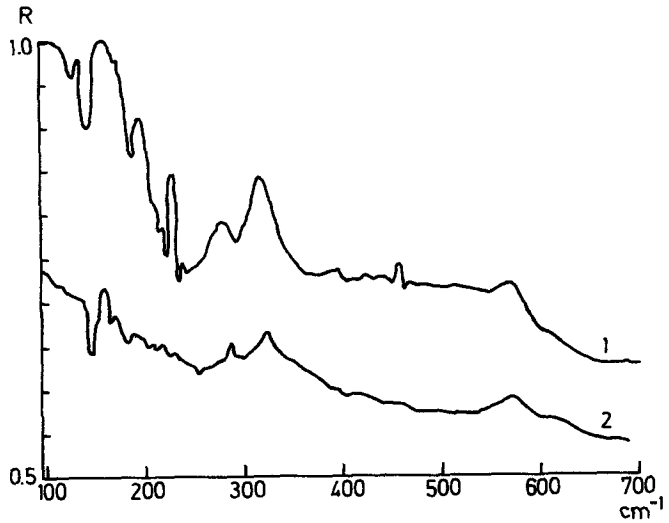

Fig. 32. Reflection spectra for $YBa_2Cu_3O_{7-y}$ at 4.2 and 300 K (the upper and lower curves, respectively).[53]

with an interaction of radiation with optically active vibrations of the crystal lattice. The nature of the 460 cm^{-1} peak is not clear: it may be connected with the electron-phonon interaction effects upon lattice vibrations.

The authors believe an essential drop in a reflection factor (40–50%) within the range 130–170 cm^{-1} is to be connected with electron excitation through a superconducting energy gap.

The value of $2\Delta/T_c$ determined by the onset of the reflectivity drop is approximately 2.5. The analogous results were obtained, for example, in Ref. 54. Optical properties of $La_{1.83}Sr_{0.17}CuO_{4-y}$ and $RBa_2Cu_3O_{7-y}$ were investigated in the frequency range $\hbar w = 0.06$–10 eV[55] at room temperature. It is shown that the typical feature of the ceramics under study is the low value of reflectivity R for $\lambda < 1$ μm and sharp increase up to 40% for $\lambda > 1.5$ μm.

Frequency dependence of the real $\varepsilon_1(w)$ and imaginary $\varepsilon_2(w)$ parts of a complex dielectric constant (Fig. 33) reveals that although the spectrum has some regions with $\varepsilon_1 \simeq 0$, the condition for plasma resonance ($\varepsilon_1 \simeq 0$, $\varepsilon_2 << 1$) does not hold due to high values of $\varepsilon_2 \simeq 6$–8.

Thus, the drop of $R(\lambda)$ observed at < 2 μm is not connected with the plasma edge. Two "zeroes" of $\varepsilon_1(w)$ at 0.6–0.8 eV (1), 0.072 eV (2) ($La_{1.83}Sr_{0.17}CuO_{4-y}$) and 0.11 eV ($SmBa_2Cu_3O_{7-y}$) are apparently due to interband transitions. In $La_{1.83}Sr_{0.17}$ CuO_{4-y}, $\varepsilon_1(w)$ has one more zero ($\hbar w = 0.059$ eV).

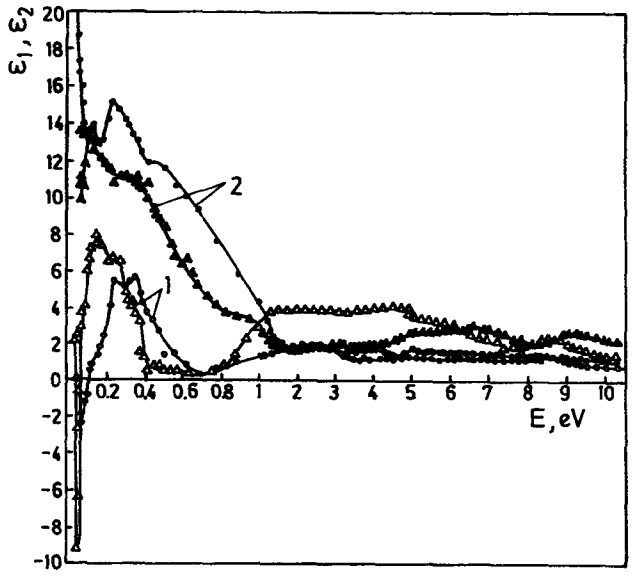

Fig. 33. Real $'_1(\chi)$ (curve 1) and imaginary $'_2(\omega)$ (curve 2) part of complex dielectric constant: $La_{1.83}Sr_{0.17}CuO_{4-y}$ (D,) and $SmBa_2Cu_2O_{7-y}$ (o, ●).[55]

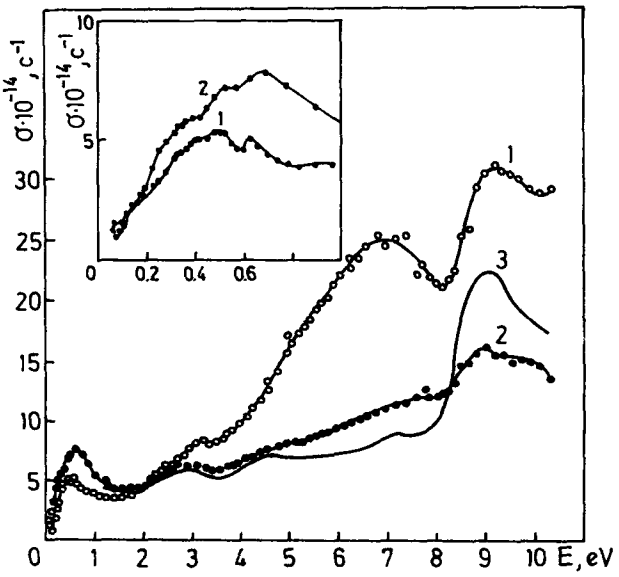

Fig. 34. Dispersion of optic permeability $\sigma(\chi)$ for $La_{183}Sr_{017}CuO_{4-y}$ (curve 1), $SmBa_2Cu_2O_{7-y}$ (curve 2) and $HoBa_2Cu_3O_{7-y}$ (curve 3).[55]

The absence of Drude behavior of optical conductivity $\rho(w)$ in the IR region (Fig. 34) indicates that within the investigated region of frequencies optical absorption is due to interband electron transitions. $La_{1.83}Sr_{0.17}CuO_{4-y}$ and $SmBa_2Cu_3O_{7-y}$ are characterized by two absorption bands: low-energy (E = 0.1–1.3 eV) and high-energy (E = 5–8 eV). The intensity of the latter sharply increases with the increase of the photon energy. It is difficult to explain the low-frequency absorption band on the basis of the available band-structure calculations for these compounds. The analogous absorption observed in Refs. 56, 57 was attributed to "charge transfer excitons". Correlation of this absorption with superconducting transition temperature T_c demonstrated in Refs. 56, 57 may be an indication of the "excitonic" mechanism of superconductivity in these systems.

2.7. *Spin-lattice relaxation in $La_{1.85}Sr_{0.15}CuO_{4-y}$ and $YBa_2Cu_3O_{4-y}$*

The discovery of high-temperature superconductivity in compounds $La_{2-x}Sr_xCuO_{4-y}$ has provoked the necessity to estimate experimentally the electron density of states at Fermi level and the energy gap appearing during the superconducting transition. These estimates may be obtained from joint analysis of temperature dependences of magnetic susceptibility and spin-lattice relaxation rate T_1^{-1} of nuclear spins for atoms, the electron states of which contribute to the total density of states at the Fermi level.

In compounds with metallic type of conductivity the value of T_1^{-1} is mainly determined by fluctuating part of hyper-fine interactions of nuclear spin with electrons from the conduction band: $(T_1T)^{-1} \sim \langle N^2(\varepsilon_F)\rangle$, where $\langle N^2(\varepsilon_F)\rangle$ is the square of the density of states at the Fermi level averaged over the interval $\sim k_B T$. Analogously magnetic susceptibility has spin contribution $\chi_{sp} \sim \langle N(\varepsilon_F)\rangle$ along with others. Joint analysis of the data on χ and T_1^{-1} allows, in a number of cases, to estimate the density of states at the Fermi level.

Spin-lattice relaxation rate was measured at frequencies 22.3 MHz (^{63}Cu) and 12.1 MHz (^{139}La).[45,58,59,78] The change in the amplitude of a spin-echo signal was registered after the change in the repetition rate of the two rf-pulses forming the echo. The amplitude of a rotating component of rf-field amounted to 0.013 T. Due to essentially wide ($> 0.1\ T$) NMR spectra the restoration of nuclear magnetization was described by a sum of exponents with constants multiple to T_1. The values of T_1 given below correspond to the flattest part of a restoration curve.

Figures 35 and 36 show temperature dependences of χ, (T_1T^{-1}) for ^{63}Cu and ^{139}La nuclei of $La_{2-x}Sr_xCuO_{4-y}$ compounds for $T > T_c$. The decrease in these values with decreasing temperature for $x < 0.2$ indicates variation of χ_{sp}. Structural transformation into orthorhombic phase observed within this range of Sr

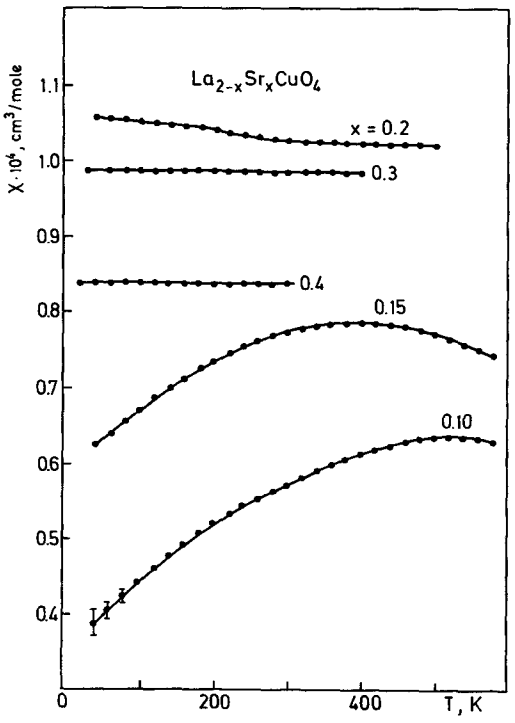

Fig. 35. Temperature dependences of magnetic susceptibility for $La_{2-x}Sr_xCuO_{4-y}$.[45]

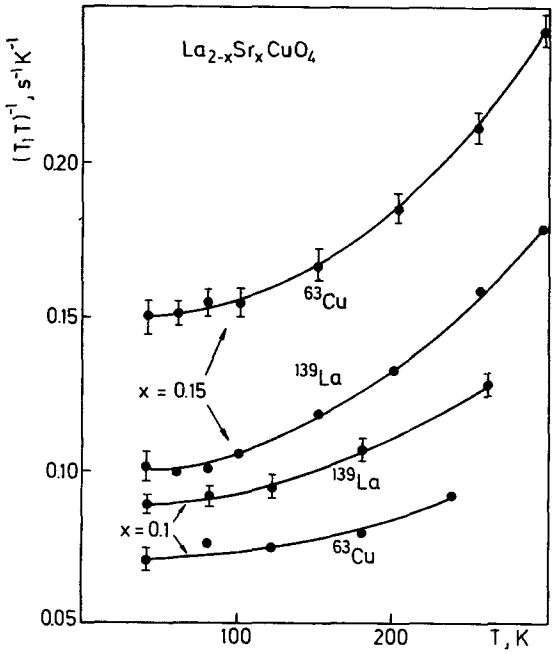

Fig. 36. Temperature dependences of $(T_1T)^{-1}$ for $La_{2-x}Sr_xCuO_{4-y}$.[45]

concentration[14] seems to be the main reason for the decrease of spin contribution. For $x \geq 0.2$ χ and $(T_1T)^{-1}$ are temperature independent.

Below critical temperature (T_c) due to "freezing" of carriers in conduction band, an exponential growth of spin-lattice relaxation time $T_1 \sim \exp(\Delta/k_B T)$ should be observed. In BCS theory $2\Delta/k_B T_c = 3.52$. This value may grow for the strong-coupling superconductors. The $La_{2-x}Sr_xCuO_{4-y}$ ($x = 0.1, 0.15, 0.2$) compounds in a superconducting state ($T < T_c$) show an exponential growth of spin-lattice relaxation time for the nuclei ^{63}Cu and ^{139}La indicating the appearance of energy gap Δ (Fig. 37). For the investigated compositions $2\Delta/k_B T_c = 3.5$–4.0 is close to that of the BCS theory. It is of interest that in the vicinity of the superconducting transition there is no Hebel-Slichter anomaly in the relaxation rate. This fact may result from a number of reasons: "dirty" limit of superconductivity, relatively large transition width, and anisotropy of the energy gap.

Temperature dependence of spin-lattice relaxation rate of ^{63}Cu was investigated in $YBa_2Cu_3O_{7-y}$ ($T_c = 87$ K, $\Delta T_c = 5$ K) in the normal and superconducting states. The measurements were carried out both in magnetic field $B=2$ T at 22.3 MHz (Fig. 37a) and in zero magnetic field at nuclear quadrupole resonance frequency of ^{63}Cu $V_Q = 31{,}5$ MHz (Fig. 37b).

In normal state the spin-lattice relaxation rate T_1 has the Korringa behavior: $(T_1T)^{-1} = 3{,}3(3)_{NMR}\ ^{-1}K^{-1}$, $(T_1T)^{-1}{}_{NQR} = 6{,}5(5)_s\ ^{-1}K_{-1}$. Magnetic susceptibility

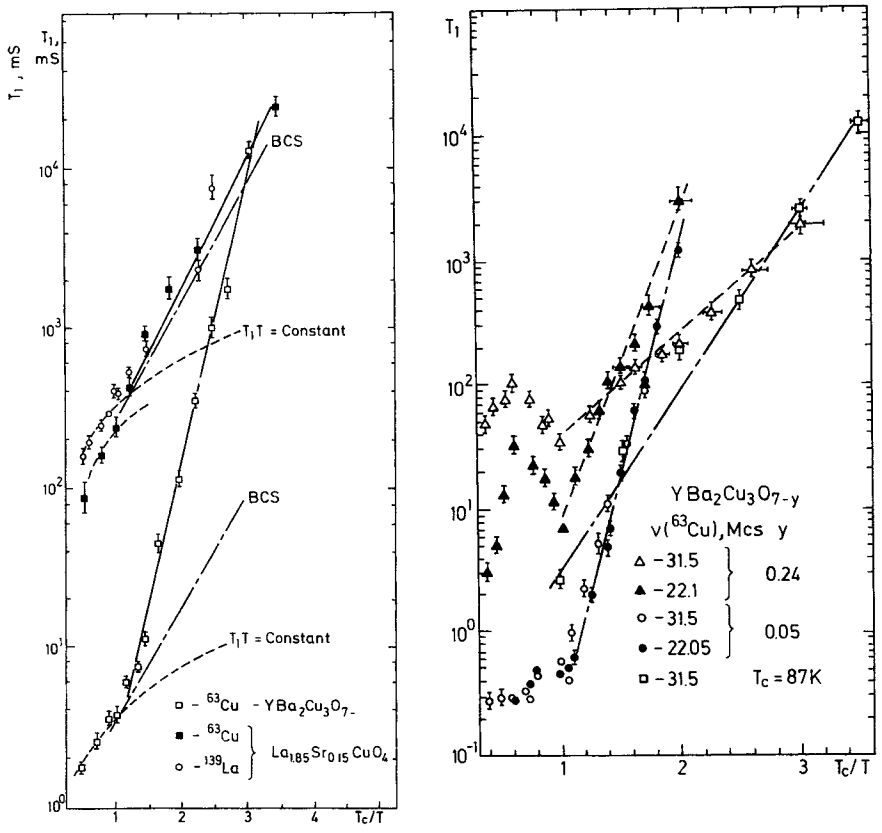

Fig. 37. (a) — temperature dependence of NMR spin-lattice relaxation time of ^{63}Cu (22, 3 MHz), ^{139}La (12, 1 MNz) for $La_{1.85}Sr_{0.15}CuO_{4-y}$ and ^{63}Cu in $YBa_2Cu_3O_{7-y}$ (T_c = 87 K, ν = 22.3 MHz, B=2 T). (b) — temperature dependence of NQR spin-lattice relaxation time of ^{63}Cu in $YBa_2Cu_3O_{7-y}$ (B=0T): y=0.05 (T_c = 93 K); • – 22.05 MHz; ○ – 31.5 MHz; y = 0.24 (T_c = 56 K); ▲ – 22.05 MHz; Δ – 31.5 MHz; T_c = 87 K; □ – 31.5 MHz.

shows the analogous temperature independent behavior. Comparing the values of $(T_1T)^{-1}_{Cu}$ in normal state for $La_{1.85}Sr_{0.15}O_{4-y}$, and Y $Ba_2Cu_3O_{7-y}$ one may conclude that in the latter $\langle N(E_f)\rangle$ is much larger and of the order of ~ 1, 5 state / EV at Cu spin.

After the superconducting transition the growth of NMR spin-lattice relaxation time essentially exceeds that expected in the BCS theory (dash-dot line in Fig. 37a). Estimates of the energy gap yield the value $2\Delta/k_B T_c$ = 8,0 (5). This points to a significant growth of pairing interaction while going from $L_{2-x}Sr_xCuO_{4-y}$ to $YBa_2Cu_3O_{4-y}$.

Measurements of T_1 were also performed in $YBa_2Cu_3O_{6.95}$ (T_c = 93 K, ΔT_c = 3 K) and $YBa_2Cu_3O_{6.76}$ (T_c = 56 K, ΔT_c = 8 K) with oxygen content (y) determined via neutron scattering and thermogravimetry, T_1, was measured for

the NQR frequencies at two lattice positions of Cu (Cu(1)-chains, Cu(2)-planes). υ(Cu1) = 22.05 MHz, υ(Cu2) = 31.5 MHz (Fig. 37b). The growth of y leads to a significant drop in the spin-lattice relaxation rate, indicating the drop in $\langle N(E_F)\rangle$. In the superconducting state the exponential growth of T_1 with lowering temperature was observed. The slope of T_1 (T_c/T) dependence shown in Fig. 37b yields the following estimates of $2\Delta/k_B T_c$: for $YBa_2Cu_3O_{6.95}$ $-\dfrac{2\Delta}{k_B T_c} =$ 12(2) (31.5MHz), 14 (2) (22.05 MHz), for $YBa_2Cu_3O_{6.76}$ $-\dfrac{2\Delta}{k_B T_c} = 3{,}7$ (5) (31,5 MHz), 9 (1) (22.05 MHz), indicating the significant drop in the values of $2\Delta/k_B T_c$ with the growth of oxygen deficits at NQR frequency of 31.5 MHz (Cu (2)-planes). For $YBa_2Cu_3O_{7-y}$ (T_c = 87 K) $- 2\Delta/k_B T_c = 7.5$ (5) at 31.5 MHz.

2.8. Disorder effects in high-temperature ceramic superconductors

Physical properties of the ordered crystals in many cases are greatly dependent upon the degree of order of a crystal lattice. That is why various methods of disordering are widely used to study what role the crystal structure plays in the formation of any of the extremal properties of a solid. Radiation disordering by fast neutron irradiation is the most "pure" method for this type of investigation. The papers 60–63, 40 report the first data on radiation effects in new ceramic superconductors $La_{1.83}Sr_{0.17}CuO_{4-y}$, $R_1Ba_2Cu_3O_{7-y}$ (R = Y, Ho, Er) irradiated by fast neutrons ($E_n \geq 1$ meV, $T_{irr} \simeq 350$ K) of fluences from 5×10^{17} to 1×10^{19} cm^{-2}. For comparison we have chosen V_3Si, the most extensively studied superconducting intermetallic compound, the physical nature of radiation effects of which is practically out of doubt.

Irradiation was carried out in a water cavity of the atomic reactor in sealed aluminium tubes placed in cadmium cases. The samples were prepared by a standard ceramic technology from copper, lanthanium or rare-earth metal oxides and carbonates of strontium and barium. Irradiation leads to a rapid decrease in T_c for all of the compounds under study. The results are shown in Figs. 38, 39, 40. It is seen from Fig. 40 that the rate of decreasing T_c with fluences in ceramic superconductors in sufficiently higher than in A-15 intermetallic compounds.

In $La_{1.83}Sr_{0.17}CuO_{4-Y}$, T_c decreases about twice at fluences of 5×18^{18} cm^{-2} while at 1×10^{19} cm^{-2} for $T \geq 1.7$ K there is no superconductivity at all. Under irradiation the width of transition markedly increases while in V_3Si it practically does not change within the same range of fluences. At small density of measuring current (5×10^{-3} A/cm^2) the resistive transition was complete, with the increase of this current "tails" appear in the irradiated samples (Fig. 38). This phenomenon as well as the behavior of dependences R (T) and H_{c2} (T) in unirradiated samples seem to be due to the granular nature of the investigated samples. This fact does not allow the correct determination of the absolute value of electric resistivity and its change under irradiation. The temperature derivative of the second critical field defined from the midpoint of the resistive transition changed

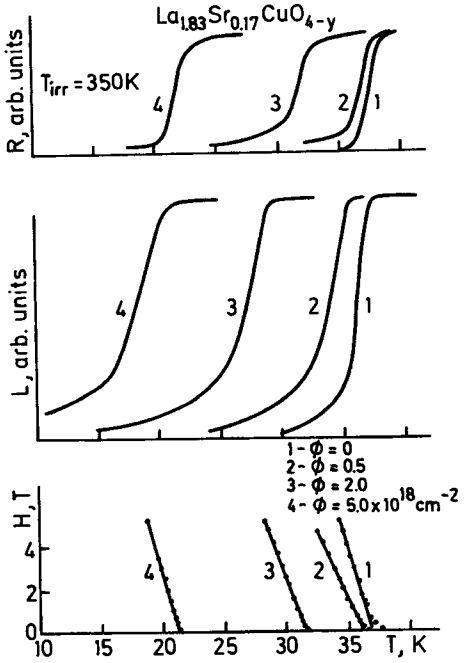

Fig. 38. Temperature dependences of electric resistance R, inductance of the measurement coil L and H_{c2} for $La_{1.83}Sr_{0.17}CuO_{4-y}$: ϕ = O (curve 1), ϕ = 0.5 (curve 2), ϕ = 2.0 (curve 3), ϕ = 5.0 × $10^{18}cm^{-2}$ (curve 4), T_{irr} = 350 K[61].

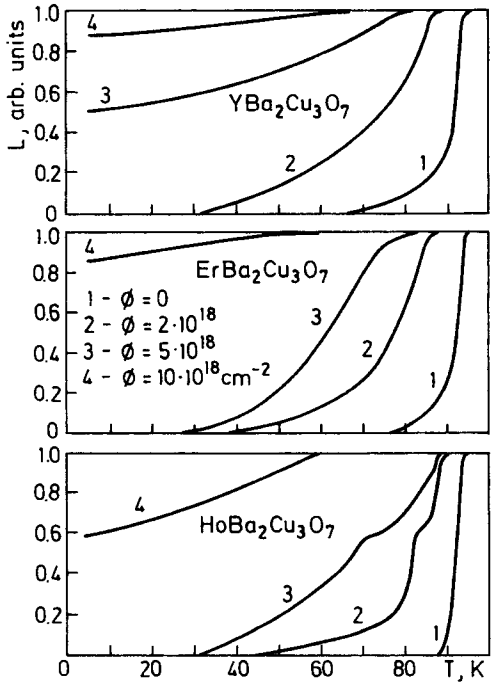

Fig. 39. Inductive transitions for $RBa_2Cu_3O_{7-y}$.[61]

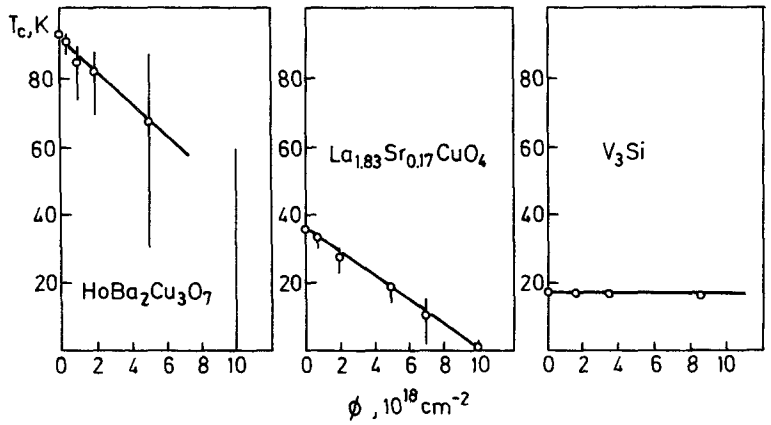

Fig. 40. Dependence of T_c and ΔT_c (vertical fractions) on fast neutron fluence.[61]

slightly with fluence. It should be noted that at comparable changes of T_c the A-15 intermetallic compounds always show an essential growth in H'_{c2}. Isochronous annealing of the sample by fluence of $1 \times 10^{19}cm^{-2}$ in air for 10 min have shown that recovering of T_c starts at 400°C and stops at 800°C.

In the $R_1Ba_2Cu_3O_{7-y}$ compounds (R = Y, Er, Ho) the onset of the superconducting transition temperature (94 K for the unirradiated samples according to inductive measurements) decreases under irradiation with about the same rate ($4\ K/10^{18}cm^{-2}$) similar to $La_{1.83}Sr_{0.17}CuO_{4-y}$. These compounds are characterized by sharper deformation of transitions compared to La-ceramics, the low-temperature part being deformed more strongly than high-temperature ones. Therefore, the narrower the transition in the initial state the less is the decrease in T_c. It is to be noted that at fluences of $5 \times 10^{18}\ cm^{-2}$ and $10 \times 10^{18}\ cm^{-2}$ the inductive transitions are not complete.

At small fluences temperature dependence of electrical resistance above T_c remains linear, while the ratio δ_{300}/δ^* decreases, for instance, in $Ho_1Ba_2Cu_3O_{7-y}$ from 2.5 to 1.8 at fluence of $2\times10^{18}\ cm^{-2}$. However, at high fluences ($2.5 \times 10^{20}cm^{-2}$) the behavior of electric resistivity changes so that at $T \geq 300$ K $\ln 1/\delta \sim T^{-1/4}$ indicating the possibility of Anderson Localization. In $RBa_2Cu_3O_{7-y}$, H'_{c2} changes much less as compared to A-15 intermetallic compounds at comparable levels of T_c degradation.[64]

Figures 41 and 42 show the neutron diffraction patterns ($\gamma = 1.513$ Å, $\Delta d/d \simeq 0.5\%$) for the samples before and after irradiation. In $La_{1.83}Sr_{0.17}CuO_{4-y}$ the absolute intensities of structural reflexes decrease slightly, their widths and relative intensities being unchanged. Oxygen occupation numbers and lattice parameters did not change within experimental error. The isotropic Debye-Waller factor did not change greatly. X-ray analysis of the sample irradiated by fluence of $5 \times 10^{19}\ cm^{-2}$ evidences an increase in the lattice parameters by 1%.

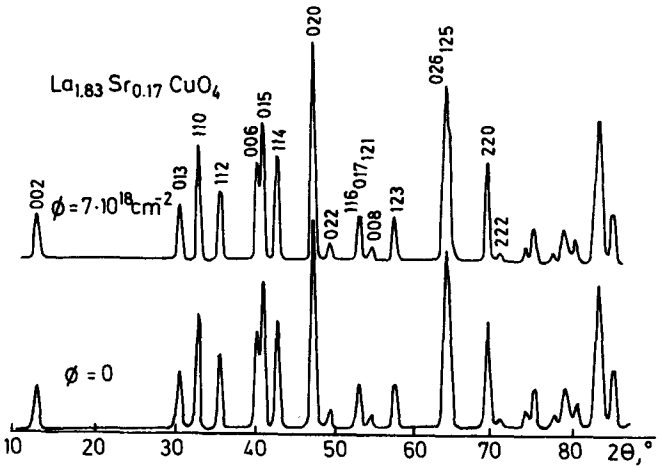

Fig. 41. Neutron diffraction patterns for $La_{1.83}Sr_{0.17}CuO_{4-y}$.[61]

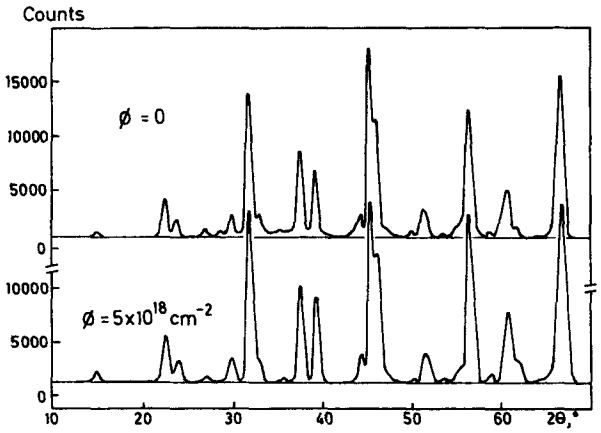

Fig. 42. Neutron diffraction patterns for Ho $Ba_2Cu_3O_{7-y}$.[61]

Even at this fluence the initial crystal structure of the type K_2NiF_4 remains (widths of reflexes and their relative intensities practically do not change). In V_3Si an essential redistribution of the V and Si atoms over the lattice sites was observed, the crystal structure being unchanged ($\phi = 5 \times 10^{19} cm^{-2}$).[64] Unlike the La system in $RBa_2Cu_3O_{7-y}$ irradiated by a fluence of 5×10^{18} cm^{-2} the variation of intensity ratio for individual reflexes, broadening of their widths, large increase in B-factor and decrease in degree of the orthorhombic lattice was observed.

We measured also the temperature dependence of heat capacity C_p for $La_{1.83}Sr_{0.17}CuO_{4-y}$ before and after irradiation by fluence of $7 \times 10^{18} cm^{-2}$ (Fig.

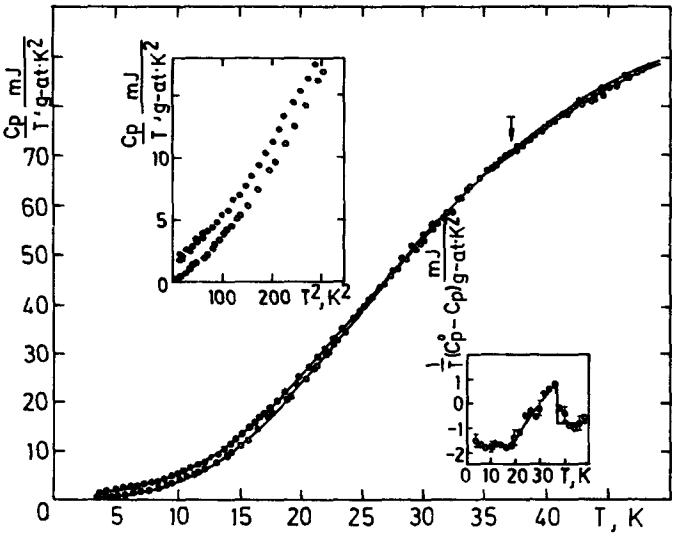

Fig. 43. Heat capacity for $La_{1.83}Sr_{0.17}CuO_{4-y}$: $\Phi = 0$ (0), $\Phi = 7 \times 10^{18} cm^{-2}$ (●), $T_{irr} = 350$ K.[61]

43). In the irradiated sample ($T_c \simeq 10$ K) the transition is very broadened and weakly seen in the dependence $C_p(T)$. The lower insertion in Fig. 43 shows the difference in heat capacities before and after irradiation within the temperature range 3–50 K.

The above structural data and the behavior of C_p versus T within 10–20 K (see the upper insertion in Fig. 43) suggest that the phonon spectrum does not change greatly under irradiation. In this case the difference in heat capacities before and after irradiation yields the temperature dependence of electronic heat capacity of the unirradiated sample (see the lower insertion in Fig. 43).

This procedure allows us to determine more accurately the value of heat capacity jump while going from normal to superconducting state $\Delta C_p/T_c = 2.0 \pm 0.2$ mJ/g-at.K^2. From the data on the lower insertion of Fig. 43, assuming that the entropies in the normal and superconducting states are equal, we obtain the value of electronic heat capacity factor for an unirradiated sample $\gamma = 0.8$ mJ/g-at.K^2.

The results obtained show that the mechanism of electron coupling in new high-temperature superconductors is more sensitive to radiation-induced distortions of a crystal structure than in the ordered systems studied previously.[64]

The low-temperature irradiation (80 K) showed that the observed effects are due to intrinsic radiation disordering and are not connected with radiation heating of the samples.

Magnetic susceptibility χ of the samples $La_{1.83}Sr_{0.17}CuO_{4-y}$ and Y $Ba_2Cu_3O_{6.95}$

irradiated by fast neutrons at $T_{irr} = 80$ K were investigated in fields of 200–7000 Oe.[77] The results are shown in Figs. 44 and 45. The temperature dependence of the susceptibility is well-described by the relation $\chi = \chi_o + \frac{C}{T-\theta}$. In the interval $0 - 2 \cdot 10^{19}\text{cm}^{-2}$ χ_{300} increases with fluence from $0.77 \times 10^{-4}\text{cm}^3/\text{mol}$ to $1.66 \times 10^{-4}\text{cm}^3/$ mol for $La_{1.83}Sr_{0.17}CuO_{4-y}$ and from $2.40 \times 10^{-4}\text{cm}^3/$ mol to $2.85 \times 10^{-4}\text{cm}^3/$ mol to $2.85 \times 10^{-4}\text{cm}^3/$ mol for Y $Ba_2Cu_3O_{6.95}$ (the values of θ are within the range 0–4 K).

Parameter C increases linearly with fluence reflecting apparently the increase in effective magnetic moment on Cu. It should be noted that steepness of the dependence $C(\phi)$ for $YBa_2Cu_3O_{6.95}$ is three times that for $La_{1.83}Sr_{0.17}CuO_{4-y}$. Since concentration of the Cu atoms in yttrium lattice is three times more than in La one, it may be suggested that during radiation disordering defects of the same type occur in the nearest surrounding of the Cu atoms.

3. Theoretical Discussion

In conclusion let us briefly discuss some possible ways of interpreting the physical properties of metal-oxide superconductors. For a more detailed summary of the available theories the reader is referred to Ref. 65. The whole complex of the available experimental data demonstrate that these systems are characterized by superconductivity of the BCS type based on the Bose-condensation of singlet Cooper pairs. The main properties of new superconductors differ slightly from those of ordinary superconductors. The most obvious differences are manifested in:

(i) unusually high values of T_c,

(ii) absence or small enough value of isotope effect in 1-2-3 system,[66–68]

(iii) rather wide distribution of data concerning the value of an energy gap.

The latter peculiarity is especially pronounced while comparing the above IR and NMR data. The main theoretical problem is apparently the understanding of the mechanism of Cooper pairing in new superconductors and explanation of the above peculiarities.

It should be noted that a number of properties of these systems in the normal state also need special explanation. It concerns, first of all, the anomalous linear temperature growth of electric resistivity. Besides, it is important to understand what role the structural instabilities (and also antiferromagnetism) play in the formation of the normal and superconducting properties. Below we only touch upon a number of these questions.

3.1. Electron-phonon interaction

In principle the T_c values in metal-oxide superconductors may be understood on the basis of a standard model for electron-phonon pairing interaction in the

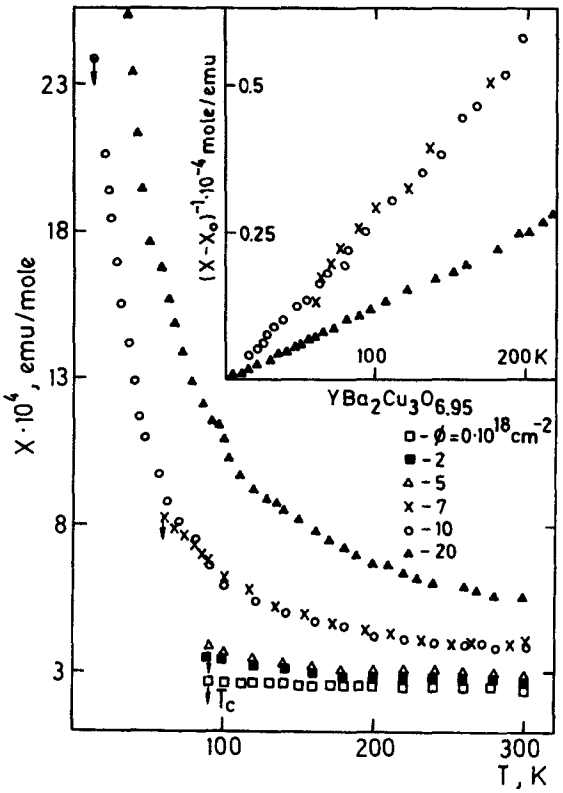

Fig. 44. Temperature dependence of magnetic susceptibility for irradiated samples of $YBa_2Cu_3O_{0,95}$.

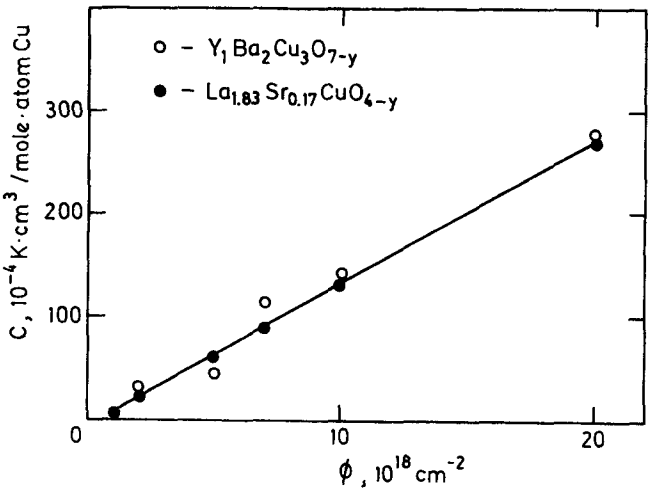

Fig. 45. Normalized Curie constant C (per Cu atom) versus fluence in $La_{1.83}Sr_{0.17}CuO_{4-y}$ and $YBa_2Cu_3O_{6.95}$.

limit of the very strong coupling. In this case T_c is well-described by Allen-Dynes interpolation formula:[69]

$$T_c = \frac{f_1 f_2}{1.20} w_{\log} \exp\left\{-\frac{1.04\,(1+\lambda)}{\lambda - \mu^*\,(1+0.62\lambda)}\right\}$$

where

$$f_1 = \left[1 + (\lambda/\lambda_1)^{3/2}\right]^{1/3}; f_2 = 1 + \frac{[\langle w^2\rangle^{1/2}/w_{\log} - 1]\lambda^2}{\lambda^2 + \lambda_2^2}$$

$$\lambda_1 = 2.46\,(1+3.8\mu^*); \lambda_2 = 1.82(1+6.3\mu^*)\frac{\langle w^2\rangle^{1/2}}{w_{\log}}.$$

Here $w_{\log}$ is the mean logarithmic frequency, $\langle w^2\rangle$ is the mean square of phonon frequency (the averaging is over the real phonon spectrum), μ^* is the Coulomb pseudopotential, λ is the dimensionless constant of pairing interaction. At $\lambda \leq 1.5$ the Allen-Dynes formula reduces to a well-known McMillan expression for T_c, while at $\lambda \geq 10$ there is a crossover to the asymptotics of the very strong coupling: $T_c \simeq 0.18\sqrt{\lambda\langle w^2\rangle}$. Using the McMillan formula for λ we have : $\lambda = N(\varepsilon_F)\langle J^2\rangle/M\langle w^2\rangle$ where $\langle J^2\rangle$ is the average matrix element of electron-phonon interaction, M is the ion mass. In this case for a maximal transition temperature we get: $T_c^{\max} \simeq 0.18\sqrt{N(\varepsilon_F)\langle J^2\rangle/M}$. For typical values characteristic of transition metal compounds $N(E_F)\langle J^2\rangle = 3$ eV/Å^2 and it follows that $T_c^{\max} \simeq$ 100 K.

Using the typical values $\langle w^2\rangle^{1/2} = 400$ K and $w_{\log} = 350$ K (which qualitatively corresponds to the above data for the phonon spectra of $La_{2-x}Sr_xCuO_{4-y}$ and $YBa_2Cu_3O_{7-y}$) and the Allen-Dynes formula, we obtain (for typical $\mu^* = 0.1$) the T_c for different values of λ (Table 3). It is seen that the values of λ slightly exceeding its value in some known[69] superconductors can explain the experimental data for T_c. Actually the high enough average frequencies of the phonon spectrum (see above) in these systems may be the reason for the observed T_c values. Additional support for this view may be obtained from the data for $2\Delta/T_c$ obtained via numerical solution of Eliashberg equations for a simplified Einstein model of the phonon spectrum.[70,71] In particular, using the above value of $w_{\log} = 350$ K and experimental value of $T_c = 37$ K for $La_{1.83}Sr_{0.17}CuO_{4-y}$ and $T_c = 95$ K for 1-2-3 system one can easily estimate (for $\mu^* = 0.1$) from $2\Delta/T_c$ versus $T_c/w_{\log}$ dependence given in Ref. 71:

$$\frac{2\Delta}{T_c} \simeq \begin{cases} 4.0\ \text{(La–Sr)} \\ 6.5\ \text{(1-2-3)} \end{cases}.$$

Table 3. T_c for different values of λ as determined by Allen-Dynes interpolation formula.

λ	0.5	1.0	1.5	2.0	2.5	3.0	3.5	4.0
T_c	4.3	26	44.5	59	71	82	91	100

These values are in surprisingly good agreement (for such a rough theory) with the quoted data for $2\Delta/T_c$ obtained for NMR relaxation measurements. Apparently these data may be considered as an evidence for the essential growth of the constant of pairing interaction λ while going from $La_{2-x}Sr_xCuO_{4-y}$ to 1-2-3 system. It should be noted that our NMR experiments essentially determine the maximal value of Δ (corresponding to maximal relaxation time). Determination of Δ from the threshold of IR absorption gives the minimal gap. Therefore, the value $2\Delta/T_c = 2.5$ for $YBa_2Cu_3O_{7-y}$ may point to an essential gap anisotropy $\Delta_{max}/\Delta_{max} = 3$, that may result from a quasi-two-dimensional character of the electron spectrum of the system under study.[20,21,44] However, this point of view cannot explain the absence of an isotope effect in 1-2-3 system.[66,67] Note, however, that the recent paper[68] reports on the observation of this effect in $YBa_2Cu_3O_{7-y}$ are anomalously small in value.

3.2 Excitonic mechanism

The simplest explanation for the absence (or negligible value) of an isotope effect along with high T_c value may be connected with the excitonic mechanism of superconductivity.[72] We think the version of this mechanism proposed for metal-oxide superconductors in Refs. 73, 74 to be the most attractive. According to this model the high T_c values are associated with charge transfer excitons $Cu^{3+}O^{2-} \rightarrow Cu^{2+}O^{-}$.

These excitons should be displayed in optical absorption spectra. It is reasonable to associate these excitons with low-energy absorption observed within the energy range 0.1–1.3 eV.[55] This viewpoint is also supported by correlation of this absorption with the value of T_c observed in Refs. 56, 57. The results of quasichemical analysis of the equilibrium of point defects in $La_{2-x}Sr_xCuO_{4-y}$ system[75,76] provide an extra evidence for this mechanism of superconductivity. From the defect structure model suggested it follows that within the range of x-0.3 non-stoichiometry $y\,x^2$. This dependence is supported by experimental data. It turns out that the Cu^{3+} ion concentration is determined by the relation $Cu^{3+} = x - kx^2$, where k depends on the oxygen pressure during the synthesis and may be obtained from the experiment. It was found that the concentration of Cu^{3+} is maximal for $x = 1/6$. It is just this composition that corresponds to maximal transition temperature (cf. Fig. 1). Direct correlation between Cu^{3+} concentration and T_c is a strong evidence for excitonic mechanism suggested in Refs. 73, 74.

Naturally, to make a final judgement in favor of this or that model for pairing interaction one needs further investigation, especially, on single crystals. It is most likely that the unique properties of these compounds are connected with a combined action of strong electron-phonon interaction and some kind of excitonic mechanism. Of course, other possibilities can not be excluded.[65]

Acknowledgments

The authors would like to express their gratitude to all of the co-authors of the above cited (and forgotten) papers of Sverdlovsk collaboration. This review could never appear without their work. The authors are also indebted to academician G.A. Mesyatz for an active support of high-T_c research in Sverdlovsk.

References

In connection with the fact that the present review dealt only with the investigations made in Sverdlovsk the list of references does not pretend to give the full scope of papers. We refer to investigations of other scientists only for the sake of comparison with our data neglecting the questions of priority etc. We apologize to the authors whom we did not quote because we are limited by the length of the text. For the same reason we cannot cite all the investigations made in Sverdlovsk. Note that the majority of them are published in the following journals: *Fizika metallov I metallovedenie, Pis'ma v JETP* and in a collection *Problemy VTS.*

1. J. G. Bednorz and K. A. Müller, *Z. Phys.* **B64** (1986) 189.
2. M. K. Wu, J. R. Ashburn, C. J. Torng, P. H. Hor, R. L. Meng, L. Cao, Z. L. Huang, Y. Q. Wang and C. W. Chu, *Phys. Rev. Lett.* **58** (1987) 908.
3. V. L. Kozhevnikov, C. M. Cheshnitskii, S. A. Davydov, V. A. Fotiev, A. E. Karkin, A. V. Mirmelshtein, A. A. Fotiev and B. N. Goshchitskii, *Fizika metallov i metallovedenie* **63** (1987) 625.
4. V. R. Galakhov, B. N. Goshchitskii, V. A. Gubanov, S. A. Davydov, Yu. F. Zhuravlyov, M. G. Zemlyanov, A. E. Karkin, V. L. Kozhevnikov, K. R. Krylov, E. Z. Kurmaev, A. T. Lonchakov, A. V. Mirmelshtein, D. L. Novikov, G. H. Panova, P. P. Parshin, A. I. Ponamaryov, A. V. Fostnikov, A. F. Prekul, M. V. Sadovskii, A. A. Fotiev, V. A. Fotiev, M. N. Khlopkin, I. M. Tzidil'kovskii, N. A. Chernoplyokov, S. M. Cheshnitskii and A. A. Shikov, *Fizika metallov i metallovedenie* **63** (1987) 829.
5. B. N. Goshchitskii, S. A. Davydov, M. G. Zemlyanov, A. E. Karkin, V. L. Kozhevnikov, A. V. Mirmelshtein, G. H. Panova, P. P. Parshin, Yu. S. Ponosov, A. A. Fotiev, M. N. Khlopkin, N. A. Chernoplyokov, S. M. Cheshnitskii and A. A. Shikov, *Fizika metallov i metallovedenie* **64** (1987) 188.
6. G. Balakrishnan, N. R. Bernhoeft, Z. A. Bowden, D. MeKpaul and A. D. Taylor, *Nature* **327** (1987).
7. A. S. Ramirez, B. Batlogg, G. Aeppli, R. J. Cava, E. Rietman, A. Goldman and G. Shirane, *Phys. Rev.* **B35** (1987) 8833.
8. I. K. Yanson, L. F. Rybalchenko, V. V. Fisun, N. L. Bobrov, M. A. Obolenskii, N. B. Brandt, V. V. Moshchalkov, Yu. D. Tret'yakov, A. R. Kaul and I. E. Graboi, *Fizika nizkikh temperatur* **13** (1987) 557.
9. B. N. Goshchitskii, S. A. Davydov, M. G. Zemlyanov, A. E. Karkin, V. L. Kozhevnikov, A. V. Mirmelshtein, G. H. Panova, P. P. Parshin, Yu. S. Ponosov, A. A. Fotiev, M. N. Khlopkin, N. A. Chernoplyokov, S. M. Cheshnitskii, A. A. Shikov and Yu. L. Shitikov, *Problemy vysokotemperaturnoi sverkhprovodimosti* **1** (Sverdlovsk, 1987) p. 255.*

10. I. S. Shaplygin, B. G. Kakhan and V. B. Lazarev, *Hzurnal neorganicheskoi khimii* **24** (1979) 1478.
11. N. Nguen, J. Choisnet, M. Hervien and B. Raveau, *J. Solid State Chem.* **39** (1981) 120.
12. J. M. Longo and P. Raccah, *J. Solid State Chem.* **6** (1973) 526.
13. J. D. Jorgensen, H. B. Schuttler, D. G. Hinks, D. W. Capone, K. Zhang, M. B. Brodsky and D. J. Scalapino, *Phys. Rev. Lett.* **58** (1987) 1024.
14. A. V. Andreev, A. N. Petrov, V. E. Naish, A. Yu, Zuev and S. V. Verkhovskii, *Fiz. metallov i metalloved.* **64** (1987) 378.
15. A. V. Andreev, A. M. Burkhanov, S. V. Verkhovskii, V. V. Gudkov, I. V. Zhestovskikh, A. Yu. Zuev, V. L. Kozhevnikov, V. E. Naish, A. N. Petrov, S. M. Podgornykh, V. E. Startsev, A. V. Tkach, V. V. Ustinov, V. A. Fotiev, S. M. Cheshnitskii and S. V. Yartsev, *Pis'ma JETP* **46** Suppl. (1987) 192.
16. W. Kang, G. Collin, M. Ribault, J. Friedel, D. Jerome, J. M. Bassat, J. P. Coutures and Ph. Odier, *J. Phys.* **48** (1987) 1181.
17. A. M. Burkhanov, V. V. Gudkov, I. V. Hzestovskikh, V. L. Kozhevnikov, V. E. Naish, S. M. Podgornykh, V. E. Startsev, A. V. Tkach, V. V. Ustinov, V. A. Fotiev, S. M. Cheshnitskii and S. V. Yartsev, *Fiz. metallov i metalloved.* **64** (1987) 397.
18. V. G. Pushin, V. V. Sagaradze, B. N. Goshchitskii, V. A. Fotiev, V. L. Kozhevnikov, V. I. Zel'dovitch, S. M. Cheshnitskii, L. I. Yurchenko, E. N. Frizen, G. A. Volkov, V. A. Zavalishin, S. P. Pavlova, V. A. Shabashov, S. M. Maltsev, B. S. Vargin and A. A. Fotiev, *Fiz. metallov i metalloved.* **64** (1987) 401.
19. V. I. Anisimov, V. R. Galakhov, E. Z. Kurmaev, M. A. Korotin, V. L. Kozhevnikov and G. V. Bazuev, *Problemy VTS* (Zarechny, Sverdlovsk, 1987) pp. 2, 40.
20. L. F. Mattheis, *Phys. Rev. Lett.* **58** (1987) 1028.
21. D. Yu, A. J. Freeman and J. H. Xu, *Phys. Rev. Lett.* **58** (1987) 1035.
22. V. L. Kozhevnikov, K. R. Krylov, A. I. Ponomarev, M. V. Sadovskii, I. M. Tzidil'kovskii and S. M. Cheshnitskii, *Fiz. metallov i metallov.* **64** (1987) 184.
23. V. L. Kozhevnikov, A. T. Lonchakov, A. A. Fotiev, I. M. Tzidil'kovskii and S. M. Cheshnitskii, *Fiz. metallov i metalloved.* **64** (1987) 191.
24. J. R. Cooper, B. Alavi, L. W. Zhon, W. P. Beyermann and C. Gruner, *Phys. Rev.* **B35** (1987) 8794.
25. M. F. Hundley, A. Zettl, A. Stacy and M. L. Cohen, *Phys. Rev.* **B35** (1987) 8800.
26. N. P. Ong, Z. Z. Wang, J. Clayhold, J. M. Tarascon, L. H. Greene and W. R. MeKinnon, *Phys. Rev.* **B35** (1987) 8807.
27. K. A. Müller, M. Takashige and J. G. Bednorz, *Phys. Rev. Lett.* **58** (1987) 1143.
28. Ya. N. Blinovskov, I. A. Leonidov, V. L. Kozhevnikov, S. M. Cheshnitskii, S. A. Davydov, A. E. Karkin, A. V. Mirmelshtein, A. A. Fotiev and B. N. Goshchitskii, *Fiz. metallov i metalloved.* **64** (1987) 338.
29. Ya. N. Blinovskov, I. A. Leonidov, V. L. Kozhevnikov, S. M. Cheshnitskii, S. A. Davydov, A. E. Karkin, A. V. Mirmelshtein, A. A. Fotiev and B. N. Goshchitskii, *Pis'ma JETP* **46** Suppl. (1987) 11.
30. R. L. Cava, B. Batlogg, R. B. van Dover, D. W. Murphy, S. Sunshine, T. Siegrist, J. P. Remeika, E. A. Rietman, S. Zahurak and G. P. Espinosa, *Phys. Rev. Lett.* **58** (1987) 1676.

*Collection "Problemy vysokotemperaturnoi sverkhprovodimosti", edited by the Ural Branch of the USSR Academy of Sciences, Sverdlovsk (1987) contains information on the Conference devoted to problems of high-temperature superconductivity, held in Zarechny (Sverdlovsk region) in 7–10 of July, 1987. It is further cited in "Problemy VTS".

31. D. W. Murphy, S. Sunshine, R. B. van Dover, R. J. Cava, B. Batlogg, S. M. Zahurak and L. F. Sehnesmeyer, *Phys. Rev. Lett.* **58** (1987) 1888.
32. P. H. Hor, R. L. Meng, Y. Q. Wang, L. Cao, Z. J. Huang, J. Bechtold, K. Foraster and C. W. Chu, *Phys. Rev. Lett.* **58** (1987) 1891.
33. Ya. N. Blinovskov, V. I. Bobrovskii, B. N. Goshchitskii, S. A. Davydov, A. E. Karkin, V. L. Kozhevnikov, I. A. Leonidov, A. V. Mirmelshtein, A. A. Podlesnyak and S. M. Cheshnitskii, *Problemy VTS* (Zarechny, Sverdlovsk, 1987) Vol. 1, p. 246.
34. O. Fisher, Special Adriatic Research Conference, Report, High-Temperature Superconductors (July 5–8, 1987, Trieste, Italy).
35. P. P. Parshin, M. G. Zemlyanov, N. A. Chernoplyokov, Yu. L. Shitikov, V. L. Kozhevnikov, S. M. Cheshnitskii, A. R. Gordeev, A. R. Kaul and I. E. Graboi, *Problemy VTS* (Zarechny, Sverdlovsk, 1987) Vol. 1, p. 257.
36. Yu. S. Ponosov, V. L. Kozhevnikov, O. V. Gurin, S. M. Cheshnitskii, G. A. Bolotin and N. K. Shindel'man, *Problemy VTS* (1987) Vol. II, p. 30.
37. A. V. Andreev, V. L. Kozhevnikov, V. E. Naish and S. M. Cheshnitskii, *Problemy VTS* (1987) 184.
38. I. F. Berger, V. I. Voronin, Yu. G. Chukalkin, V. R. Shtirts, A. E. Ermakov, V. V. Maikov, Ya. N. Blinovskov, S. A. Davydov, A. E. Karkin, V. L. Kozhevnikov, I. A. Leonidov, A. V. Mirmelshtein, M. V. Sadovskii, S. M. Cheshnitskii and B. N. Goshchitskii, *Fiz. metallov i metalloved.* **64** (1987) 394.
39. I. F. Berger, V. I. Voronin, Yu. G. Chukalkin, V. R. Shtirts, A. V. Ermakov, V. V. Maikov, Ya. N. Blinovskov, V. I. Bobrovskii, S. A. Davydov, A. E. Karkin, V. L. Kozhevnikov, I. A. Leonidov, A. V. Mirmelshtein, M. V. Sadovskii, S. M. Cheshnitskii and B. N. Goshchitskii, *Pis'ma JETP* **46** Suppl. (1987) 22.
40. I. F. Berger, Ya. N. Blinovskov, V. I. Voronin, B. N. Goshchitskii, V. L. Kozhevnikov, I. A. Leonidov and S. M. Cheshnitskii, *Problemy VTS* (1987) Vol. 1, p. 80.
41. T. Siegrist, S. Sunshine, D. W. Murphy, R. J. Cava and S. M. Zahurak, *Phys. Rev.* **B35** (1987) 7137.
42. J. Capponi, C. Chaillout, A. W. Hewat, P. Lejay, M. Marezio, N. Nguen, B. Raveau, J. L. Soubeyrouk, J. L. Tholence and R. Tournier, *Europhys. Lett.* **3** (1987) 1301.
43. N. M. Chebotaev, A. A. Samokhvalov, S. V. Naumov, V. A. Kostylev and B. A. Gizhevskii, *Problemy VTS* (1987) Vol. 1, p. 103.
44. L. F. Mattheis, D. R. Hamann, *Solid State Commun.* **63** (1987) 395.
45. B. A. Aleksashin, S. V. Verkhovskii, B. N. Goshchitskii, A. Yu. Derevskov, A. Yu. Zuev, V. L. Kozhevnikov, V. L. Konstantinov, K. R. Krylov, A. T. Lonchakov, K. N. Mikhalyov, A. N. Petrov, A. I. Ponomarev, M. V. Sadovskii, I. M. Tsidil'kovskii, V. I. Tsidil'kovskii, S. M. Cheshnitskii, *Pis'ma JETP* **46** Suppl. (1987) 51.
46. V. L. Kozhevnikov, A. T. Lonchakov, V. I. Tsidil'kovskii, I. M. Tsidil'kovskii and S. M. Cheshnitskii, *Problemy VTS* (Zarechny, Sverdlovsk, 1987) Vol. II, p. 52.
47. L. Z. Avdeev, N. B. Brandt, A. V. Volkozub, V. V. Moshchalkov, O. V. Snigiryov, A. A. Gippius, I. E. Graboi, A. R. Kaul, I. G. Muttik, Yu. D. Tret'yakov, R. V. Shpanchenko and V. V. Khanin, *Problemy VTS* (1987) Vol. II, p. 146.
48. N. V. Anshukova, A. I. Golovashkin, A. K. Zvezdin, Z. A. Kazei, R. Z. Levitin, B. V. Mill, K. V. Mitsen, V. V. Snegiryov and V. I. Sokolov, *Problemy VTS* (1987) Vol. II, p. 152.
49. H. R. Ott, Report at the Special Adriatico Research Conference on High-Temperature Superconductors (July 5–8, 1987, Trieste, Italy).
50. J. O. Willis, Z. Fisk, J. D. Thompson, S. W. Cheong, R. M. Aikin, J. L. Smith and E. Zirngiebl, *JMMM* **67** (1987) L139.
51. B. D. Dunlap, M. Slaski, D. G. Hinks, L. Soderholm, M. Beno, K. Zhang, C. Segre, G.

W. Crabtree, W. K. Kwok, S. K. Malik, I. K. Schuller, J. D. Jorgensen and Z. Sungalia, Preprint Argonne Nat. Lab. (1987) *JMMM* (in press).
52. B. D. Dunlap, M. Slaski, Z. Sungalia, D. G. Hinks, K. Zhang, C. Segre, S. K. Malik and E. E. Alp, Preprint Argonne Nat. Lab. (1987).
53. A. Yu. Derevskov, V. L. Kozhevnikov, V. L. Konstantinov, I. M. Tsidil'kovskii and S. M. Cheshnitskii, *Problemy VTS* (1987) Vol. II, p. 5.
54. D. A. Bonn, J. E. Greedan, C. V. Stager, T. Timusk, M. G. Doss, S. L. Herr, K. Kamaras and D. B. Tanner, *Phys. Rev. Lett.* **58** (1987) 2249.
55. L. V. Nomerovannaya, M. M. Kirillova, V. L. Kozhevnikov, N. V. Minulina and S. M. Cheshnitskii, *Problemy VTS* (1987) Vol. II, p. 26.
56. K. Kamaras, C. D. Porter, M. G. Doss, S. L. Herr, D. B. Tanner, D. A. Bonn, J. E. Greelan, A. H. O. Reilly, C. V. Stager and T. Timusk, *Phys. Rev. Lett.* **59** (1987) 919.
57. S. Etemad, D. E. Aspnes, M. K. Kelly, R. Thompson, J. M. Tarascon and C. M. Hull, Preprint Bell Comm. Research (1987).
58. B. A. Aleksashin, S. V. Verkhovskii, K. N. Mikhalyov, B. N. Goschitskii, A. N. Petrov, V. L. Kozhevnikov, A. Yu. Zuev and S. M. Cheshnitskii, *Fiz. metallov i metalloved.* **64** (1987) 392.
59. B. A. Aleksashin, K. N. Mikhalyov, S. V. Verkhovskii, B. N. Goshchitskii, V. L. Kozhevnikov, S. M. Cheshnitskii, L. Ya. Gavrilova and A. Yu. Zuev, *Problemy VTS* (1987) Vol. I, p. 201.
60. V. I. Voronin, S. A. Davydov, A. E. Karkin, A. V. Mirmelshtein, V. L. Kozhevnikov, S. M. Cheshnitskii, V. A. Fotiev, V. D. Parkhomenko and B. N. Goshchitskii, *Pis'ma JETP* **46** Suppl. (1987) 165.
61. B. N. Goshchitskii, S. A. Davydov, A. E. Karkin, A. V. Mirmelshtein, V. D. Parkhomenko, V. I. Voronin, V. L. Kozhevnikov and S. M. Cheshnitski, Conference on New Mechanisms of Superconductivity, Report (June, 1987, Berkeley, USA).
62. S. A. Davydov, A. E. Karkin, A. V. Mirmelshtein, V. L. Kozhevnikov, S. M. Cheshnitskii, V. A. Fotiev, V. D. Parkhomenko and B. N. Goshchitski, *Fiz. metallov i metalloved.* **64** (1987) 399.
63. I. F. Berger, V. I. Voronin, B. N. Goshchitskii, S. A. Davydov, A. E. Karkin, V. L. Kozhevnikov, A. V. Mirmelshtein, V. D. Parkhomenko, S. M. Cheshnitskii, Yu. G. Chukalkin and V. R. Shtirts, *Problemy VTS* (1987) Vol. II, p. 204.
64. B. N. Goshchitskii, V. E. Arkhipov, Yu. G. Chukalkin, Soviet Sci. Reviews in *Physics. Reviews.* **8** (1987) 520, Harwood Academic Publ. NY.
65. T. M. Rice, *Z. Phys.* **B67** (1987) 141.
66. B. Batlogg, R. J. Cava, A. Jaryaraman, R. B. Van Dover, G. A. Kourouklis, S. Sunshine, D. W. Murphy, L. W. Rupp, H. S. Chen, A. T. Short, A. M. Mujsce and E. A. Rietman, *Phys. Rev. Lett.* **58** (1987) 2333.
67. L. C. Bourne, M. F. Crommie, A. Zettl, H. C. Zurloye, S. W. Keller, K. L. Leary, A. M. Stacy, K. J. Chang, M. L. Cohen and D. E. Morns, *Phys. Rev. Lett.* **58** (1987) 2337.
68. K. L. Leary *et al.*, *Phys. Rev. Lett.* **59** (1987) 1236.
69. P. B. Allen and R. C. Dynes, *Phys. Rev.* **B12** (1975) 905.
70. J. P. Carbotte, F. Marsiglio and B. Mitrovic, *Phys. Rev.* **B33** (1986) 6135.
71. F. Marsiglio and J. P. Carbotte, *Solid. State Commun.* **63** (1987) 419.
72. Problema vysokotemperaturnoi sverkhprovodimosti, eds. V. L. Ginzburg and D. A. Kirzhnits, *Nauka*, M. 1977.
73. C. M. Varma, S. Schmitt-Rink and E. Abrahams, Preprint Bell Labs., *Solid. State Commun.* (1987).
74. C. M. Varma, S. S. Schmitt-Rink and E. Abrahams, Special Adriatico Research Conference on High-Temperature Superconductors Report (July 5–8, 1987, Trieste, Italy).

75. Ya. N. Blinovskov, I. A. Leonidov, S. A. Davydov, A. V. Mirmelshtein, A. E. Karkin, I. A. Kanteeva, B. S. Kogan, K. M. Demchuk, B. I. Kamenetskii, S. M. Cheshnitskii and V. L. Kozhevnikov, *Problemy VTS* (1987) Vol. I, p.4
76. I. A. Leonidov, Ya. N. Blinovskov, V. B. Vykhodets, S. M. Klotsman, A. D. Levin, S. M. Cheshnitskii and V. L. Kozhevnikov, *Problemy VTS* (1987) Vol. I, p. 72.
77. K. N. Mikhalyov, Yu. I. Zhdanov, B. A. Aleksashin, S. V. Verkhovskii, B. N. Goshchitskii, S. A. Davydov, A. V. Mirmelstein and A. E. Karkin, *Pis'ma JETP* (in press).
78. B. A. Aleksashin, Yu. I. Zhdanov, S. V. Verkhovskii, K. N. Mikhalyov and V. V. Serikov, *Pis'ma JETP* (1988), to be published.